EUROPEAN ORGANIZATION FOR NUCLEAR RESEARCH (CERN)

CERN-PH-EP/2010-055
2010/12/26

CMS-BPH-10-003

Upsilon production cross section in pp collisions at $\sqrt{s} = 7$ TeV

The CMS Collaboration*

Abstract

The Y production cross section in proton-proton collisions at $\sqrt{s} = 7$ TeV is measured using a data sample collected with the CMS detector at the LHC, corresponding to an integrated luminosity of $3.1 \pm 0.3\,\mathrm{pb}^{-1}$. Integrated over the rapidity range $|y| < 2$, we find the product of the $\Upsilon(1S)$ production cross section and branching fraction to dimuons to be $\sigma(\mathrm{pp} \to \Upsilon(1S)X) \cdot \mathcal{B}(\Upsilon(1S) \to \mu^+\mu^-) = 7.37 \pm 0.13^{+0.61}_{-0.42} \pm 0.81\,\mathrm{nb}$, where the first uncertainty is statistical, the second is systematic, and the third is associated with the estimation of the integrated luminosity of the data sample. This cross section is obtained assuming unpolarized $\Upsilon(1S)$ production. If the $\Upsilon(1S)$ production polarization is fully transverse or fully longitudinal the cross section changes by about 20 %. We also report the measurement of the $\Upsilon(1S)$, $\Upsilon(2S)$, and $\Upsilon(3S)$ differential cross sections as a function of transverse momentum and rapidity.

Submitted to Physical Review D

*See Appendix A for the list of collaboration members

1 Introduction

The hadroproduction of quarkonia is not understood. None of the existing theories successfully reproduces both the differential cross section and the polarization measurements of the J/ψ or Y states [1]. It is expected that studying quarkonium hadroproduction at higher center-of-mass energies and over a wider rapidity range will facilitate significant improvements in our understanding. Measurements of the Y resonances are particularly important since the theoretical calculations are more robust than for the charmonium family, due to the heavy bottom quark and the absence of b-hadron feed-down. Measurements of quarkonium hadroproduction cross sections and production polarizations made at the Large Hadron Collider (LHC) will allow important tests of several alternative theoretical approaches. These include non-relativistic QCD (NRQCD) factorization [2], where quarkonium production includes color-octet components, and calculations made in the color-singlet model including next-to-leading order (NLO) corrections [3] which reproduce the differential cross sections measured at the Tevatron experiments [4, 5] without requiring a significant color-octet contribution.

This paper presents the first measurement of the $\Upsilon(1S)$, $\Upsilon(2S)$, and $\Upsilon(3S)$ production cross sections in proton-proton collisions at $\sqrt{s} = 7\,\text{TeV}$, using data recorded by the Compact Muon Solenoid (CMS) experiment between April and September 2010. In these measurements the signal efficiencies are determined with data. Consequently, Monte Carlo simulation is used only in the evaluation of the geometric and kinematic acceptances. The document is organized as follows. Section 2 contains a short description of the CMS detector. Section 3 presents the data collection, the online and offline event selections, the Y reconstruction, and the Monte Carlo simulation. The detector acceptance and efficiencies to reconstruct Y events in CMS are discussed in Sections 4 and 5, respectively. In Section 6 the fitting technique employed to extract the cross section is presented. The evaluation of systematic uncertainties on the measurements is described in Section 7. Section 8 presents the $\Upsilon(nS)$ cross section results and comparisons to existing measurements at lower collision energies [4, 5] and to the PYTHIA [6] event generator.

2 The CMS detector

The central feature of the CMS apparatus is a superconducting solenoid, of 6 m inner diameter, providing a field of 3.8 T. Inside the solenoid in order of increasing distance from the interaction point are the silicon pixel and strip tracker, the crystal electromagnetic calorimeter, and the brass/scintillator hadron calorimeter. Muons are detected by three types of gas-ionization detectors embedded in the steel return yoke: drift tubes (DT), cathode strip chambers (CSC), and resistive plate chambers (RPC). The muon measurement covers the pseudorapidity range $|\eta| < 2.4$, where $\eta = -\ln[\tan(\theta/2)]$ and the polar angle θ is measured from the z-axis, which points along the counterclockwise beam direction. The silicon tracker is composed of pixel detectors (three barrel layers and two forward disks on either side of the detector, made of 66 million $100 \cdot 150\,\mu\text{m}^2$ pixels), followed by microstrip detectors (ten barrel layers plus three inner disks and nine forward disks on either side of the detector, with 10 million strips of pitch between 80 and 184 μm). Due to the strong magnetic field and the fine granularity of the silicon tracker, the transverse momentum, p_{T}, of the muons matched to silicon tracks is measured with a resolution of about 1% for a typical muon in this analysis. The silicon tracker also provides the primary vertex position with $\sim 20\,\mu$m accuracy. The first level (L1) of the CMS trigger system, composed of custom hardware processors, uses information from the calorimeters and muon detectors to select the most interesting events. The high-level trigger (HLT) further decreases the event rate before data storage. A more detailed description of the CMS detector can be found elsewhere [7].

3 Data sample and event reconstruction

3.1 Event selection

The data sample used in this analysis was recorded by the CMS detector in ppcollisions at a center-of-mass energy of 7 TeV. The sample corresponds to a total integrated luminosity of $3.1 \pm 0.3\,\mathrm{pb}^{-1}$ [8]. The maximum instantaneous luminosity was $10^{31}\,\mathrm{cm}^{-2}\,\mathrm{s}^{-1}$ and event pileup was negligible. Data are included in the analysis if the silicon tracker, the muon detectors, and the trigger were performing well and the luminosity measurement was available.

The trigger requires the detection of two muons at the hardware level, without any further selection at the HLT. The coincidence of two muon signals without an explicit p_{T} requirement is sufficient to maintain the dimuon trigger without prescaling. All three muon systems – DT, CSC, and RPC – take part in the trigger decision.

Anomalous events arising from beam-gas interactions or beam scraping in the beam transport system near the interaction point, which produce a large number of hits in the pixel detector, are removed with offline software filters [9]. A good primary vertex is also required, as defined in Ref. [9]. The detector systems are aligned and calibrated using LHC collision data and cosmic-ray muons [10].

3.2 Monte Carlo simulation

Simulated events are used to tune the selection criteria and to compare with data. Upsilon events are produced using PYTHIA 6.412 [6], which generates events based on the leading-order color-singlet and octet mechanisms, with NRQCD matrix elements tuned by comparing calculations with the CDF data [11] and applying the normalization and wavefunctions as recommended in Ref. [12]. The generation of $\Upsilon(2S)$ and $\Upsilon(3S)$ states has been included by changing the relevant particle masses and branching ratios. The simulation includes the generation of χ_b states. Final-state radiation (FSR) is implemented using PHOTOS [13, 14]. The response of the CMS detector is simulated with a GEANT 4-based [15] Monte Carlo (MC) program. The simulated events are processed with the same reconstruction algorithms as used for data.

3.3 Offline muon reconstruction

In this analysis, a muon is defined as a track reconstructed in the silicon tracker and associated with a compatible signal in the muon detectors. Tracks are reconstructed using a Kalman filter technique which starts from hits in the pixel system and extrapolates outward to the silicon strip tracker. The tracks found in the silicon tracker are propagated to the muon system and required to be matched to at least one muon segment in one muon station. Further details may be found in Ref. [16].

Quality criteria are applied to the tracks to reject muons from kaon and pion decays. The tracks are required to have at least twelve hits in the silicon tracker, at least one of which must be in the pixel detector, and a track-fit χ^2 per degree of freedom smaller than five. In addition the tracks are required to emanate from a cylinder of radius 2 mm and length 50 cm centered on the pp interaction region and parallel to the beam line. The muons are required to satisfy:

$$p_{\mathrm{T}}^{\mu} > 3.5\,\mathrm{GeV}/c \quad \text{if} \quad |\eta^{\mu}| < 1.6\,, \quad \text{or} \quad p_{\mathrm{T}}^{\mu} > 2.5\,\mathrm{GeV}/c \quad \text{if} \quad 1.6 < |\eta^{\mu}| < 2.4\,. \tag{1}$$

These kinematic criteria are chosen to ensure that the trigger and muon reconstruction efficiencies are high and not rapidly changing within the acceptance window of the analysis.

The momentum measurement of charged tracks in the CMS detector is affected by systematic uncertainties caused by imperfect knowledge of the magnetic field, the amount of material, and sub-detector misalignments, as well as by biases in the algorithms which fit the track trajectory. A mismeasurement of the track momentum results in a shift and broadening of the reconstructed peaks of dimuon resonances. An improved understanding of the CMS magnetic field, detector alignment, and material budget was obtained from cosmic-ray muon and LHC collision data [10, 17, 18], and the residual effects are determined by studying the dependence of the reconstructed J/ψ dimuon invariant-mass distribution on the muon kinematics [19]. The transverse momentum corrected for the residual scale distortion is parameterized as $p_{\mathrm{T}} = (1 + a_1 + a_2\eta^2) \cdot p'_{\mathrm{T}}$, where p'_{T} is the measured muon transverse momentum, $a_1 = (3.8 \pm 1.9) \cdot 10^{-4}$, and $a_2 = (3.0 \pm 0.7) \cdot 10^{-4}$. The coefficients for terms linear in η and quadratic in p'_T and $p'_T \cdot \eta$ are consistent with zero and are not included.

3.4 Υ event selection

To identify events containing an Υ decay, muons with opposite charges are paired, and the invariant mass of the muon pair is required to be between 8 and 14 GeV/c^2. The longitudinal separation between the two muons at their points of closest approach to the beam axis is required to be less than 2 cm. The two muon helices are fit with a common vertex constraint, and events are retained if the fit χ^2 probability is larger than 0.1%. The dimuon candidate is confirmed offline to have passed the trigger requirements. If multiple dimuon candidates are found in the same event, the candidate with the best vertex quality is retained; the fraction of signal candidates rejected by this requirement is about 0.2%. Finally, the rapidity, y, of the Υ candidates is required to satisfy $|y| < 2$ because the acceptance diminishes rapidly at larger rapidity. The rapidity is defined as $y = \frac{1}{2} \ln\left(\frac{E+p_{\parallel}}{E-p_{\parallel}}\right)$, where E is the energy and $p_{\parallel}$ the momentum parallel to the beam axis of the muon pair.

The dimuon invariant-mass spectrum in the $\Upsilon(nS)$ region for the dimuon transverse momentum interval $p_{\mathrm{T}} < 30$ GeV/c is shown in Fig. 1 for the pseudorapidity intervals $|\eta^{\mu}| < 2.4$ (left) and $|\eta^{\mu}| < 1.0$ (right). We obtain a Υ(1S) mass resolution of 96 ± 2 MeV/c^2 including muons from the entire pseudorapidity range, and 69 ± 2 MeV/c^2 when both muons satisfy $|\eta^{\mu}| < 1$. The observed resolutions, determined as a parameter of the fit function described in Section 6, are in good agreement with the predictions from MC simulation.

4 Acceptance

The $\Upsilon \to \mu^+\mu^-$ acceptance of the CMS detector is defined as the product of two terms. The first is the fraction of upsilons of given p_{T} and y such that each of the two muons satisfies Eq. (1). The second is the probability that each muon can be reconstructed in the tracker using the CMS software, in the absence of further event activity in the detector and without quality cuts imposed. Both components are evaluated by simulation and parametrized as a function of the p_{T} and rapidity of the Υ.

The acceptance is calculated from the ratio

$$\mathcal{A}^{\Upsilon}(p_{\mathrm{T}}, y) = \frac{N^{\Upsilon}_{\mathrm{rec}}(p_{\mathrm{T}}, y)}{N^{\Upsilon}_{\mathrm{gen}}(p_{\mathrm{T}}, y)}\,, \tag{2}$$

where $N^{\Upsilon}_{\mathrm{gen}}(p_{\mathrm{T}}, y)$ is the number of upsilons generated in a (p_{T}, y) bin, while $N^{\Upsilon}_{\mathrm{rec}}(p_{\mathrm{T}}, y)$ is the number reconstructed in the same (p_{T}, y) region but now using the reconstructed, rather than

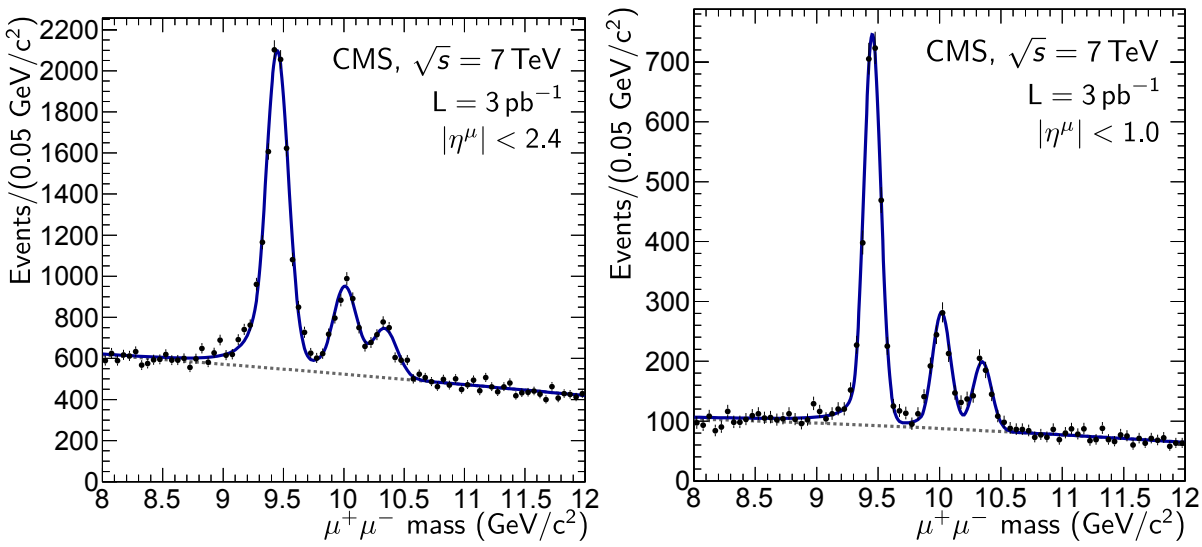

Figure 1: The dimuon invariant-mass distribution in the vicinity of the $\Upsilon(nS)$ resonances for the full rapidity covered by the analysis (left) and for the subset of events where the pseudo-rapidity of each muon satisfies $|\eta^{\mu}| < 1$ (right). The solid line shows the result of a fit to the invariant-mass distribution before accounting for acceptance and efficiency, with the dashed line denoting the background component. Details of the fit are described in Section 6.

generated, variables. In addition, the numerator requires that the two muons reconstructed in the silicon tracker satisfy Eq. (1).

The acceptance is evaluated with a signal MC sample in which the Y decay to two muons is generated with the EVTGEN [20] package including the effects of final-state radiation. There are no particles in the event besides the Y, its daughter muons, and final-state radiation. The upsilons are generated uniformly in p_{T} and rapidity. This sample is then fully simulated and reconstructed with the CMS detector simulation software to assess the effects of multiple scattering and finite resolution of the detector. The acceptance is calculated for two-dimensional (2-D) bins of size ($1\,\mathrm{GeV}/c \cdot 0.1$) in the reconstructed p_{T} and y of the Y and used in candidate-by-candidate yield corrections.

The 2-D acceptance map for unpolarized $\Upsilon(1\mathrm{S})$ is shown in the left plot of Fig. 2. The acceptance varies with the resonance mass. This is shown in the right plot of Fig. 2, which displays the acceptance integrated over the rapidity range as a function of p_{T} for each upsilon resonance. The transverse-momentum threshold for muon detection, especially in the forward region, is small compared to the upsilon mass. Therefore, when the Y decays at rest, both muons are likely to reach the muon detector. When the Y has a modest boost, the probability is greater that one muon will be below the muon detection threshold and the acceptance decreases until the Y transverse momentum reaches about $5\,\mathrm{GeV}/c$, after which the acceptance rises slowly. The production polarization of the Y strongly influences the muon angular distributions and is expected to change as a function of p_{T}. In order to account for this, the acceptance is calculated for five extreme polarization scenarios [21]: unpolarized and polarized longitudinally and transversely with respect to two different reference frames. The first is the helicity frame (HX), defined by the flight direction of the Y in the center-of-mass system of the colliding beams. The second is the Collins-Soper (CS) frame [22], defined by the bisection of the incoming proton directions in the Y rest frame.

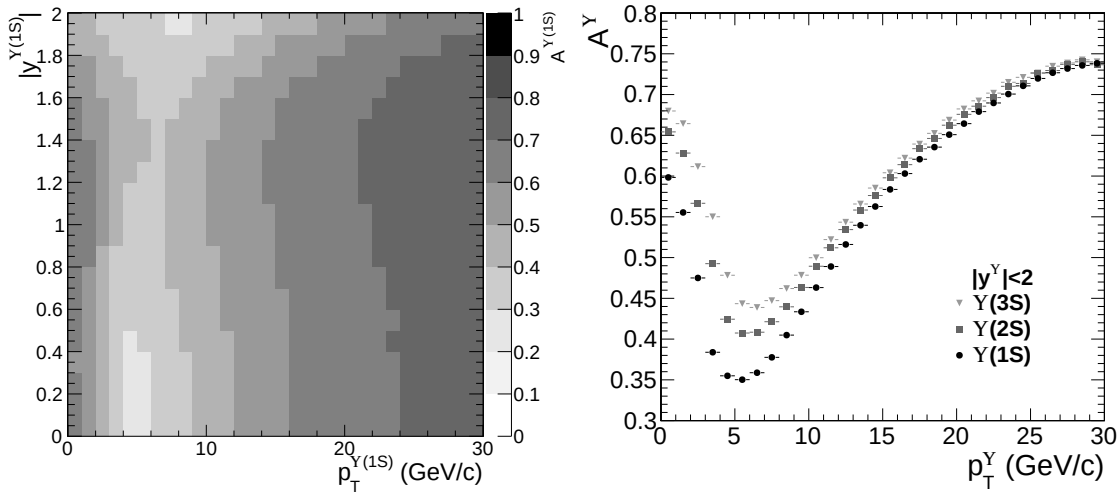

Figure 2: (Left) Unpolarized $\Upsilon(1S)$ acceptance as a function of p_T and y; (Right) the unpolarized $\Upsilon(1S)$, $\Upsilon(2S)$, and $\Upsilon(3S)$ acceptances integrated over rapidity as a function of p_T.

5 Efficiency

We factor the total muon efficiency into three conditional terms,

$$\varepsilon(\text{total}) = \varepsilon(\text{trig}|\text{id}) \cdot \varepsilon(\text{id}|\text{track}) \cdot \varepsilon(\text{track}|\text{accepted}) \equiv \varepsilon_{\text{trig}} \cdot \varepsilon_{\text{id}} \cdot \varepsilon_{\text{track}} \,. \tag{3}$$

The tracking efficiency, $\varepsilon_{\text{track}}$, combines the efficiency that the accepted track of a muon from the $\Upsilon(nS)$ decay is reconstructed in the presence of other activity in the silicon tracker, as determined with a track-embedding technique [23], and the efficiency for the track to satisfy quality criteria, as determined with the tag-and-probe (T&P) technique [23] described below. The muon identification efficiency, ε_{id}, is the probability that the track in the silicon tracker is identified as a muon. It has been computed as described in Ref. [16] and is also based on the T&P method. The efficiency that an identified muon satisfies the trigger, $\varepsilon_{\text{trig}}$, is again measured with the same technique.

The tag and probe technique is a data-based method used in this analysis to determine the track quality, muon trigger, and muon identification efficiencies. It utilizes dimuons from J/ψ decays to provide a sample of probe objects. A well-identified muon, the tag, is combined with a second object in the event, the probe, and the invariant mass is computed. The tag-probe pairs are divided into two samples, depending on whether the probe satisfies or not the criteria for the efficiency being evaluated. The two tag-probe mass distributions contain a J/ψ peak. The integral of the peak is the number of probes that satisfy or fail to satisfy the imposed criteria. The efficiency parameter is extracted from a simultaneous unbinned maximum-likelihood fit to both mass distributions.

The J/ψ resonance is utilized for T&P efficiency measurements as it provides a large-yield and statistically-independent dimuon sample [24]. To avoid trigger bias, events containing a tag and probe pair have been collected with triggers that do not impose requirements on the probe from the detector subsystem related to the efficiency measurement. For the track-quality efficiency measurement, the trigger requires two muons at L1 in the muon system without using the silicon tracker. For the muon-identification and trigger efficiencies, the trigger requires a muon at the HLT, that is matched to the tag, paired with a silicon track of opposite sign and the invariant mass of the pair is required to be in the vicinity of the J/ψ mass.

The component of the tracking efficiency measured with the track-embedding technique is well

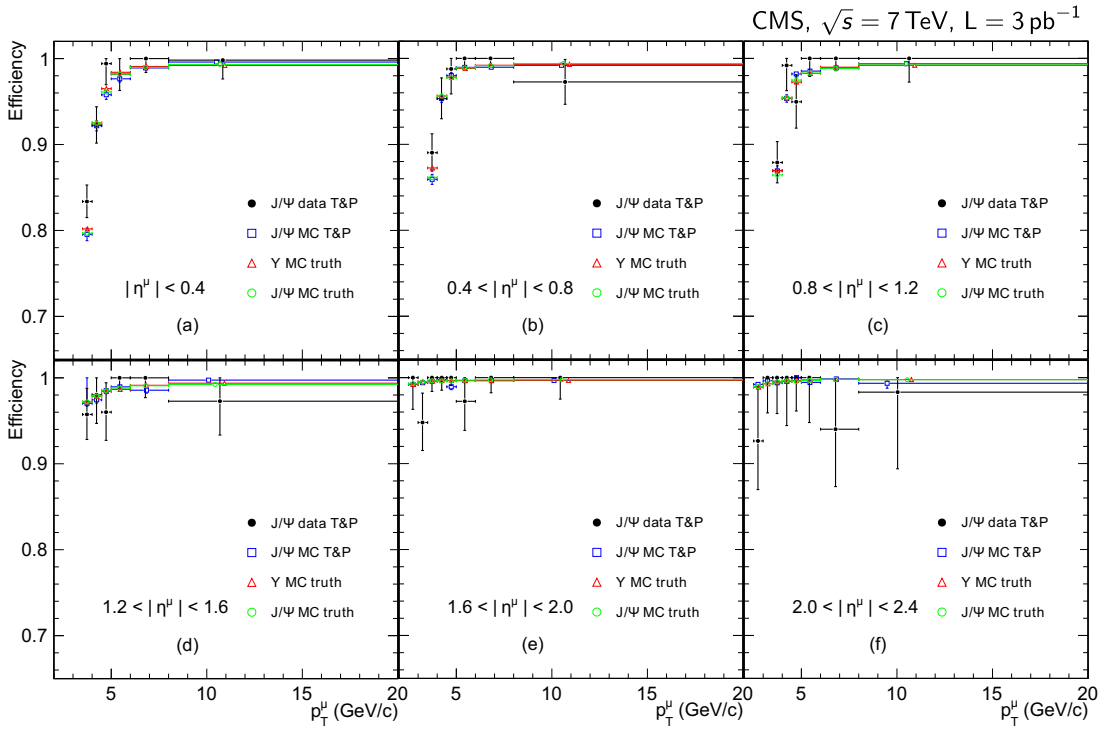

Figure 3: Single-muon identification efficiencies as a function of p_{T}^{μ} for six $|\eta^{\mu}|$ regions, measured from data using J/ψ T&P (closed circles). The efficiencies determined with Υ MC truth (triangles), J/ψ MC truth (open circles), and J/ψ MC T&P (squares), used in the evaluation of systematic uncertainties, are also shown.

Table 1: Single-muon identification efficiencies, in percent, measured from J/ψ data with T&P. The statistical uncertainties in the least significant digits are given in parentheses; uncertainties less than 0.05 are denoted by 0. For asymmetric uncertainties the positive uncertainty is reported first.

p_T^μ	$\lvert\eta^\mu\rvert$					
(GeV/c)	0.0–0.4	0.4–0.8	0.8–1.2	1.2–1.6	1.6–2.0	2.0–2.4
2.5–3.0					100(0,4)	94(6)
3.0–3.5					95(3)	100(0,4)
3.5–4.0	83(2)	89(2)	88(2)	96(3)	100(0,2)	100(0,4)
4.0–4.5	92(2)	95(2)	99(1,3)	98(2,3)	100(0,2)	100(0,6)
4.5–5.0	99(1,2)	99(1,3)	95(3)	96(3)	100(0,2)	100(0,4)
5.0–6.0	98(2)	100(0,1)	100(0,2)	100(0,1)	97(3)	100(0,5)
6.0–8.0	100(0,2)	100(0,1)	100(0,1)	100(0,2)	100(0,2)	94(6,7)
8.0–50.0	100(0,2)	97(3)	100(0,3)	97(3,4)	100(0,3)	98(2,9)

Table 2: Single-muon trigger efficiencies, in percent, measured from J/ψ data with T&P. The statistical uncertainties in the least significant digits are given in parentheses; uncertainties less than 0.05 are denoted by 0. For asymmetric uncertainties the positive uncertainty is reported first.

p_T^μ	$\lvert\eta^\mu\rvert$					
(GeV/c)	0.0–0.4	0.4–0.8	0.8–1.2	1.2–1.6	1.6–2.0	2.0–2.4
2.5–3.0					93(1)	92(2)
3.0–3.5					94(1)	93(1)
3.5–4.0	69(1)	81(1)	78(1)	98(1)	94(1)	97(1)
4.0–4.5	79(1)	91(1)	86(1)	98(1)	92(1)	96(1)
4.5–5.0	85(1)	95(1)	87(1)	97(1)	96(1)	99(1)
5.0–6.0	90(1)	97(1)	85(1)	99(0,1)	95(1)	96(1)
6.0–8.0	92(1)	97(1)	85(1)	100(0)	97(1)	99(1)
8.0–50.0	92(1)	97(1)	86(1)	99(1)	97(1)	99(2)

described by a constant value of $(99.64 \pm 0.05)\%$. The efficiency of the track-quality criteria measured by the T&P method is likewise nearly uniform and has an average value of $(98.66 \pm 0.05)\%$. Tracks satisfying the quality criteria are the probes for the muon identification study. The resulting single-muon identification efficiencies as a function of p_{T}^μ for six $|\eta^\mu|$ regions are shown in Fig. 3 and Table 1. The probes that satisfy the muon identification criteria are in turn the probes for the study of the trigger efficiency. The resulting trigger efficiencies for the same p_{T}^μ and $|\eta^\mu|$ regions are shown in Fig. 4 and Table 2.

Figures 3 and 4 also show single-muon identification and trigger efficiencies, respectively, determined from a high-statistics MC simulation. The single-muon efficiencies determined with the T&P technique in the data are found to be consistent, within the uncertainties and over

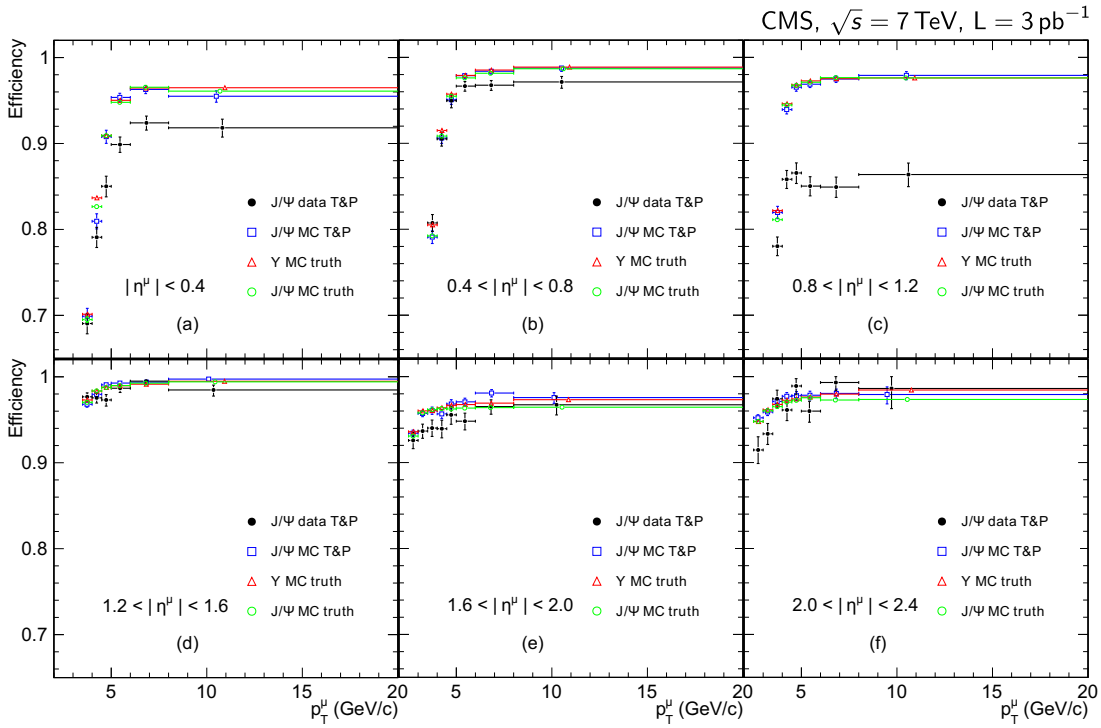

Figure 4: Single-muon trigger efficiencies as a function of p_{T}^{μ} for six $|\eta^{\mu}|$ regions, measured from data using J/ψ T&P (closed circles). The efficiencies determined with Y MC truth (triangles), J/ψ MC truth (open circles), and J/ψ MC T&P (squares), used in the evaluation of systematic uncertainties, are also shown.

most of the kinematic range of interest, with the efficiencies obtained from the Y MC simulation utilizing the generator-level particle information ("MC truth"). Two exceptions are the single-muon trigger efficiency for the intervals $|\eta^{\mu}| < 0.4$ and $0.8 < |\eta^{\mu}| < 1.2$, where the efficiency is lower in data than in the MC simulation. In both cases the MC simulation is known to not fully reproduce the detector properties or performance: gaps in the DT coverage ($|\eta^{\mu}| < 0.4$) and suboptimal timing synchronization between the overlapping CSC and DT subsystems ($0.8 < |\eta^{\mu}| < 1.2$). For all cases the data-determined efficiencies are used to obtain the central results.

The Y efficiency is estimated from the product of single-muon efficiencies. Differences between the single and dimuon efficiencies determined from MC truth and those measured with the T&P technique can arise from the kinematic distributions of the probes and from bin averaging. This is evaluated by comparing the single-muon and dimuon efficiencies as determined using the T&P method in J/$\psi \to \mu^+\mu^-$ MC events to the efficiencies obtained in the same events utilizing generator-level particle information. In addition, effects arising from differences in the kinematic distributions between the Y and J/ψ decay muons are investigated by comparing the efficiencies determined from Y $\to \mu^+\mu^-$ MC events to those from J/$\psi \to \mu^+\mu^-$ MC events. In all cases the differences in the efficiency values are not significant, and are used only as an estimate of the associated systematic uncertainties.

The efficiency of the vertex χ^2 probability cut is determined using the high-statistics J/ψ data sample, to which the Y selection criteria are applied. The efficiency is extracted from a simultaneous fit to the dimuon mass distribution of the passing and failing candidates. It is found to be $(99.2 \pm 0.1)\%$. A possible difference between the efficiency of the vertex χ^2 probability cut for the J/ψ and Y is evaluated by applying the same technique to large MC signal samples of

each resonance. No significant difference in the efficiencies is found. The efficiency of the remaining selection criteria listed in Section 3 is studied in data and MC simulation and is found to be consistent with unity.

6 Measurement of the cross sections

The $\Upsilon(nS)$ differential cross section is determined from the signal yield, $N^{\rm fit}$, obtained directly from a weighted fit to the dimuon invariant-mass spectrum, after correcting for the acceptance ($\mathcal{A}$) and the total efficiency (ε), through the equation

$$\frac{d^2\sigma\left(\mathrm{pp}\to\Upsilon(nS)X\right)}{dp_{\rm T}\,dy}\cdot\mathcal{B}\left(\Upsilon(nS)\to\mu^+\mu^-\right) \tag{4}$$

$$=\frac{\mathrm{N}^{\rm fit}_{\Upsilon(nS)}(\mathcal{A},\varepsilon)}{\mathcal{L}\,\cdot\Delta p_{\rm T}\cdot\Delta y}\,, \tag{5}$$

upon normalization by the integrated luminosity of the dataset, $\mathcal{L}$, and by the bin widths, $\Delta p_{\rm T}$ and Δy, of the Υ transverse momentum and rapidity.

The $\Upsilon(1S)$, $\Upsilon(2S)$, and $\Upsilon(3S)$ yields are extracted via an extended unbinned maximum likelihood fit. The measured mass-lineshape of each Υ state is parameterized by a "Crystal Ball" (CB) function [25]; this is a Gaussian resolution function with the low side tail replaced with a power law describing FSR. The resolution, given by the Gaussian standard deviation, is a free parameter in the fit but is constrained to scale with the ratios of the resonance masses. The FSR tail is fixed to the MC shape. Since the three resonances overlap in the measured dimuon mass, we fit the three $\Upsilon(nS)$ states simultaneously. Therefore, the probability distribution function (PDF) describing the signal consists of three CB functions. The mass of the $\Upsilon(1S)$ is a free parameter in the fit, to accommodate a possible bias in the momentum scale calibration. The number of free parameters is reduced by fixing the $\Upsilon(2S)$ and $\Upsilon(3S)$ mass differences, relative to the $\Upsilon(1S)$, to their world average values [26]. A second-order polynomial is chosen to describe the background in the 8–14 GeV/c^2 mass-fit range.

The fit to the dimuon invariant-mass spectrum, before accounting for acceptance and efficiencies, is shown in Fig. 1 for the Υ transverse momentum interval $p_{\rm T} < 30\,\mathrm{GeV}/c$, and for the fifteen $p_{\rm T}$ intervals used for the $\Upsilon(1S)$ differential cross-section measurement in Fig. 5. The observed $\Upsilon(nS)$ signal yields are reported in Table 3. The width of the $p_{\rm T}$ intervals chosen for each resonance reflects the corresponding available signal statistics. In all cases the quoted uncertainty is statistical. As shown in Table 3, for each resonance the sum of the yields in each $p_{\rm T}$ interval is consistent with the yield determined from a fit to the entire $p_{\rm T}$ range. Given the significant η and $p_{\rm T}$ dependencies of the efficiencies and acceptances of the muons from $\Upsilon(nS)$ decays, we correct for them on a candidate-by-candidate basis before performing the mass fit to obtain $N^{\rm fit}$ in Eq. (4). Specifically: an Υ candidate reconstructed with $p_{\rm T}$ and y from muons with $p_{\rm T}^{\mu_{1,2}}$ and $\eta^{\mu_{1,2}}$ is corrected with a weight

$$w \equiv w_{\rm acc}\cdot w_{\rm track}\cdot w_{\rm id}\cdot w_{\rm trig}\cdot w_{\rm misc} \tag{6}$$

where the factors are: (i) acceptance, $w_{\rm acc} = 1/\mathcal{A}^{\Upsilon}(p_{\rm T},y)$; (ii) tracking, $w_{\rm track} = 1/\varepsilon^2_{\rm track}$; (iii) identification, $w_{\rm id} = 1/\left[\varepsilon_{\rm id}(p_{\rm T}^{\mu_1},\eta^{\mu_1})\cdot\varepsilon_{\rm id}(p_{\rm T}^{\mu_2},\eta^{\mu_2})\right]$; (iv) trigger, $w_{\rm trig} = 1/\left[\varepsilon_{\rm trig}(p_{\rm T}^{\mu_1},\eta^{\mu_1})\cdot\varepsilon_{\rm trig}(p_{\rm T}^{\mu_2},\eta^{\mu_2})\right]$; and (v) additional selection criteria, $w_{\rm misc}$, including the efficiency of the vertex selection criteria. The acceptance depends on the resonance mass; the $\Upsilon(3S)$ gives rise to higher-momenta

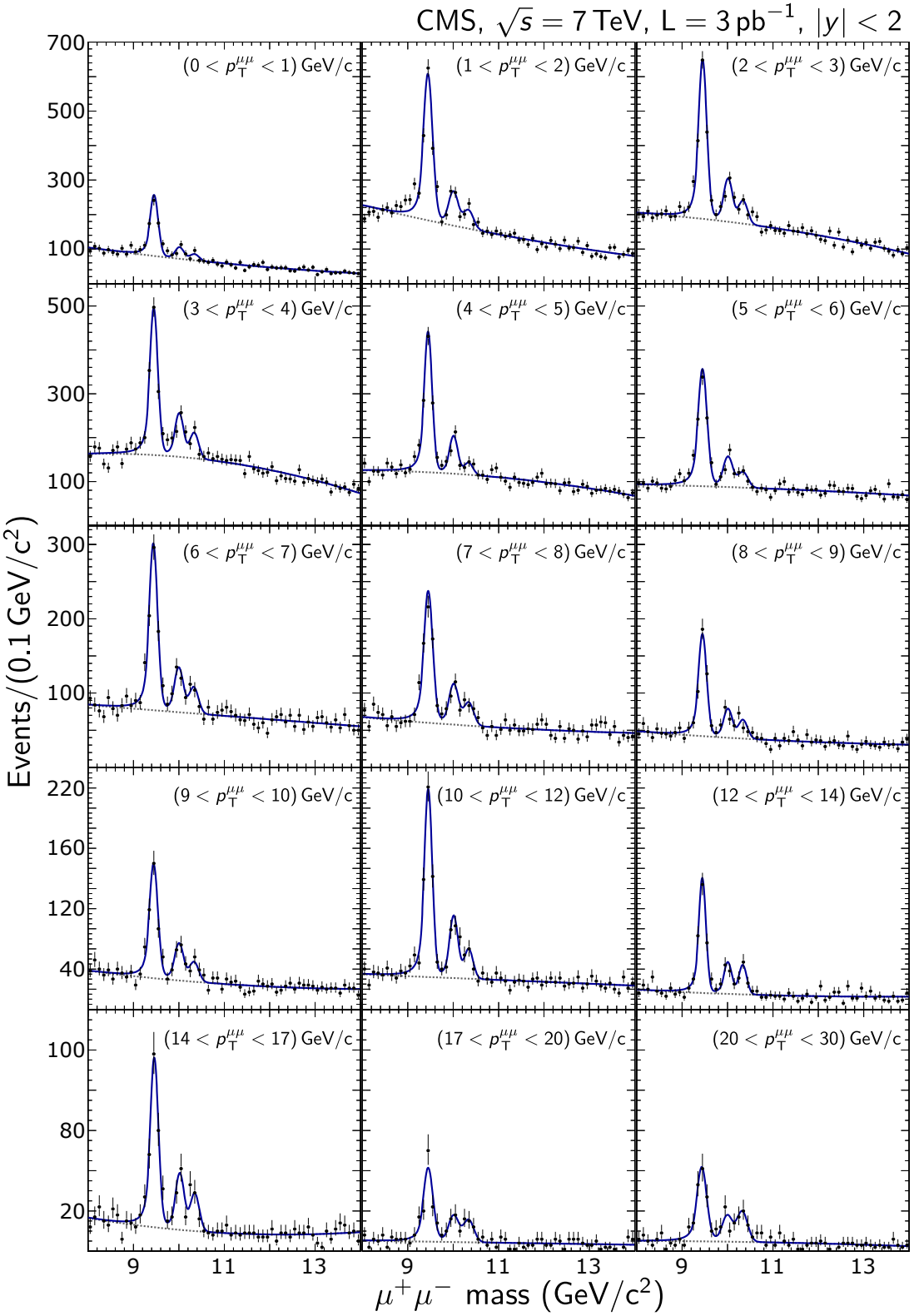

Figure 5: Fit to the dimuon invariant-mass distribution in the specified p_T regions for $|y| < 2$, before accounting for acceptance and efficiency. The solid line shows the result of the fit described in the text, with the dashed line representing the background component.

muons which results in a roughly 10% larger acceptance for the $\Upsilon(3S)$ than for the $\Upsilon(1S)$. Consequently, the corrected yield for each of the $\Upsilon(nS)$ resonances is obtained from a fit in which the corresponding $\Upsilon(nS)$ acceptance is employed.

We determine the $\Upsilon(nS)$ differential cross section using the above procedure separately for each polarization scenario. The results are summarized in Table 4. We also divide the data into two ranges of rapidity, $|y| < 1$ and $1 < |y| < 2$, and repeat the fits to obtain the $\Upsilon(nS)$ differential cross sections reported in Table 5. The integrated cross section for each resonance is obtained from the corresponding sum of the differential cross sections. The results for the $\Upsilon(1S)$ p_T-integrated, rapidity-differential cross section are shown in Table 6.

7 Systematic uncertainties

Systematic uncertainties are described in this section, together with the methods used in their determination. We give a representative value for each uncertainty in parentheses.

We determine the cross section using acceptance maps corresponding to five different polarization scenarios, expected to represent extreme cases. The values of the cross section obtained vary by about 20%. The variations depend on p_T thus affecting the shapes of the p_T spectrum.

The statistical uncertainties on the acceptance and efficiencies – single-muon trigger and muon ID, quality criteria, tracking and vertex quality – give rise to systematic uncertainties in the cross-section measurement. We vary the dimuon event weights in the fit coherently by $\pm 1\sigma(\text{stat.})$. The muon identification and trigger efficiencies are varied coherently when estimating the associated systematic uncertainties (8%).

The selection criteria requiring the muons to be consistent with emanating from the same primary vertex are fully efficient. This has been confirmed in data and simulation. The selection of one candidate per event using the largest vertex probability also has an efficiency consistent with unity. We assign an uncertainty (0.2%) from the frequency of occurrence of signal candidates in the data that are rejected by the largest vertex probability requirement but pass all the remaining selection criteria. The muon charge misassignment is estimated to be less than 0.01% [27] and contributes a negligible uncertainty.

Final-state radiation is incorporated into the simulation using the PHOTOS algorithm. To estimate the systematic uncertainty associated with this procedure, the acceptance is calculated without FSR and 20% of the difference is taken as the uncertainty based on a study in Ref. [14] (0.8%).

The definition of acceptance used in this analysis requires that the muons from the Y decay produce reconstructible tracks. The kinematic selection is applied to the reconstructed p_T and η values of these tracks. Uncertainties on the measurement of track parameters also affect the acceptance as a systematic uncertainty. The dominant uncertainty is associated with the measurement of the track transverse momentum. The acceptance is sensitive to biases in track momentum and to differences in resolution between the simulated and measured distributions. The magnitude of these effects is quantified by comparing measurements of resonance mass and width between simulation and data [19]. To determine the effect on the Y acceptance, we introduce a track p_T bias of 0.2%, chosen to be four times the maximum momentum scale residual bias after calibration (0.3%). We also vary the transverse momentum resolution by $\pm 10\%$, corresponding to the uncertainty in the resolution measurement using J/ψ, and recalculate the acceptance map (0.1%).

Imperfect knowledge of the production p_T spectrum of the Y resonances at $\sqrt{s} = 7\,\text{TeV}$ contributes a systematic uncertainty. The Y MC sample used for the acceptance calculation, Eq. (2), was generated flat in p_T, whereas the p_T spectrum in the data peaks at a few GeV/c, and behaves as a power law above 5 GeV/c. To study the effect of this difference, we have re-weighted the sample in p_T to more closely describe the expected distribution in data based on a fit to the spectrum obtained from PYTHIA (1%).

The distribution of the z position of the ppinteraction point influences the acceptance. We have produced MC samples of $\Upsilon(nS)$ at different positions along the beam line, between -10 and $+10$ cm with respect to the center of the nominal collision region (1%).

High-statistics MC simulations were performed to compare T&P single-muon and dimuon efficiencies to the actual MC values for both the Y and J/ψ, see Figs. 3 and 4. The differences and their associated uncertainties are taken as a source of systematic uncertainty. The contributions are: possible bias in the T&P technique (0.1%), differences in the J/ψ and Y kinematics (1%), and taking the product of single-muon efficiencies as an estimate of the double-muon Y efficiencies (1.6%).

MC trials of the fitter demonstrate that it is consistent with providing an unbiased estimate of the yield of each resonance, its mass, and the mass resolution (1%). A systematic variation may arise from differences between the dimuon invariant-mass distribution in the data and in the PDFs chosen for the signal and background components in the fit. We consider the following variations in the signal PDF. As the CB parameters which describe the radiative tail of each resonance are fixed from MC simulation in the nominal fit to the data, we vary the CB parameters by three times their uncertainties (3%). We also remove the resonance mass difference constraint in the p_T integrated fit (0.6%). We vary the background PDF by replacing the polynomial by a linear function, while restricting the fit to the mass range 8–12 GeV/c^2 (3% when fitting the full p_T and y ranges, varying with differential interval).

The determination of the integrated luminosity normalization is made with an uncertainty of 11% [8]. The relative systematic uncertainties from each source are summarized in Table 7 for the full rapidity range, for two rapidity ranges in Table 8, and for five rapidity ranges in Table 9. The largest sources of systematic uncertainty arise from the statistical precision of the T&P determination of the efficiencies from the data and from the luminosity normalization which dominates.

8 Results and discussion

The analysis of the collision data acquired by the CMS experiment at $\sqrt{s} = 7\,\text{TeV}$, corresponding to an integrated luminosity of $3.1 \pm 0.3\,\text{pb}^{-1}$, yields a measurement of the $\Upsilon(nS)$ integrated production cross sections for the range $|y| < 2$:

$$\sigma(\text{pp} \to \Upsilon(1\text{S})X) \cdot \mathcal{B}(\Upsilon(1\text{S}) \to \mu^+\mu^-) = 7.37 \pm 0.13(\text{stat.})^{+0.61}_{-0.42}(\text{syst.}) \pm 0.81(\text{lumi.})\,\text{nb}\,,$$

$$\sigma(\text{pp} \to \Upsilon(2\text{S})X) \cdot \mathcal{B}(\Upsilon(2\text{S}) \to \mu^+\mu^-) = 1.90 \pm 0.09(\text{stat.})^{+0.20}_{-0.14}(\text{syst.}) \pm 0.24(\text{lumi.})\,\text{nb}\,, \quad (7)$$

$$\sigma(\text{pp} \to \Upsilon(3\text{S})X) \cdot \mathcal{B}(\Upsilon(3\text{S}) \to \mu^+\mu^-) = 1.02 \pm 0.07(\text{stat.})^{+0.11}_{-0.08}(\text{syst.}) \pm 0.11(\text{lumi.})\,\text{nb}\,. \quad (8)$$

The $\Upsilon(1\text{S})$ and $\Upsilon(2\text{S})$ measurements include feed-down from higher-mass states, such as the χ_b family and the $\Upsilon(3\text{S})$. These measurements assume unpolarized $\Upsilon(nS)$ production. Assumptions of fully-transverse or fully-longitudinal polarizations change the cross sections by about

20%. The p_{T}-differential $\Upsilon(nS)$ cross sections for the rapidity intervals $|y| < 1$, $1 < |y| < 2$, and $|y| < 2$ are shown in Fig. 6. The p_{T} dependence of the cross section in the two exclusive rapidity intervals is the same within the uncertainties. The $\Upsilon(1\mathrm{S})$ p_{T}-integrated, rapidity-differential cross sections are shown in the left plot of Fig. 7. The cross section shows a slight decline towards $|y| = 2$, consistent with the expectation from PYTHIA. The ratios of $\Upsilon(nS)$ cross sections differential in p_{T} are reported in Table 10 and shown in the right plot of Fig. 7. The uncertainty associated with the luminosity determination cancels in the computation of the ratios. Both ratios increase with p_{T}. In Fig. 8 the differential cross sections for the $\Upsilon(1\mathrm{S})$, $\Upsilon(2\mathrm{S})$, and $\Upsilon(3\mathrm{S})$ are compared to PYTHIA. The normalized p_{T}-spectrum prediction from PYTHIA is consistent with the measurements, while the integrated cross section is overestimated by about a factor of two. We have not included parameter uncertainties in the PYTHIA calculation. We do not compare our measurements to other models as no published predictions exist at $\sqrt{s} = 7\,\mathrm{TeV}$ for Υ production.

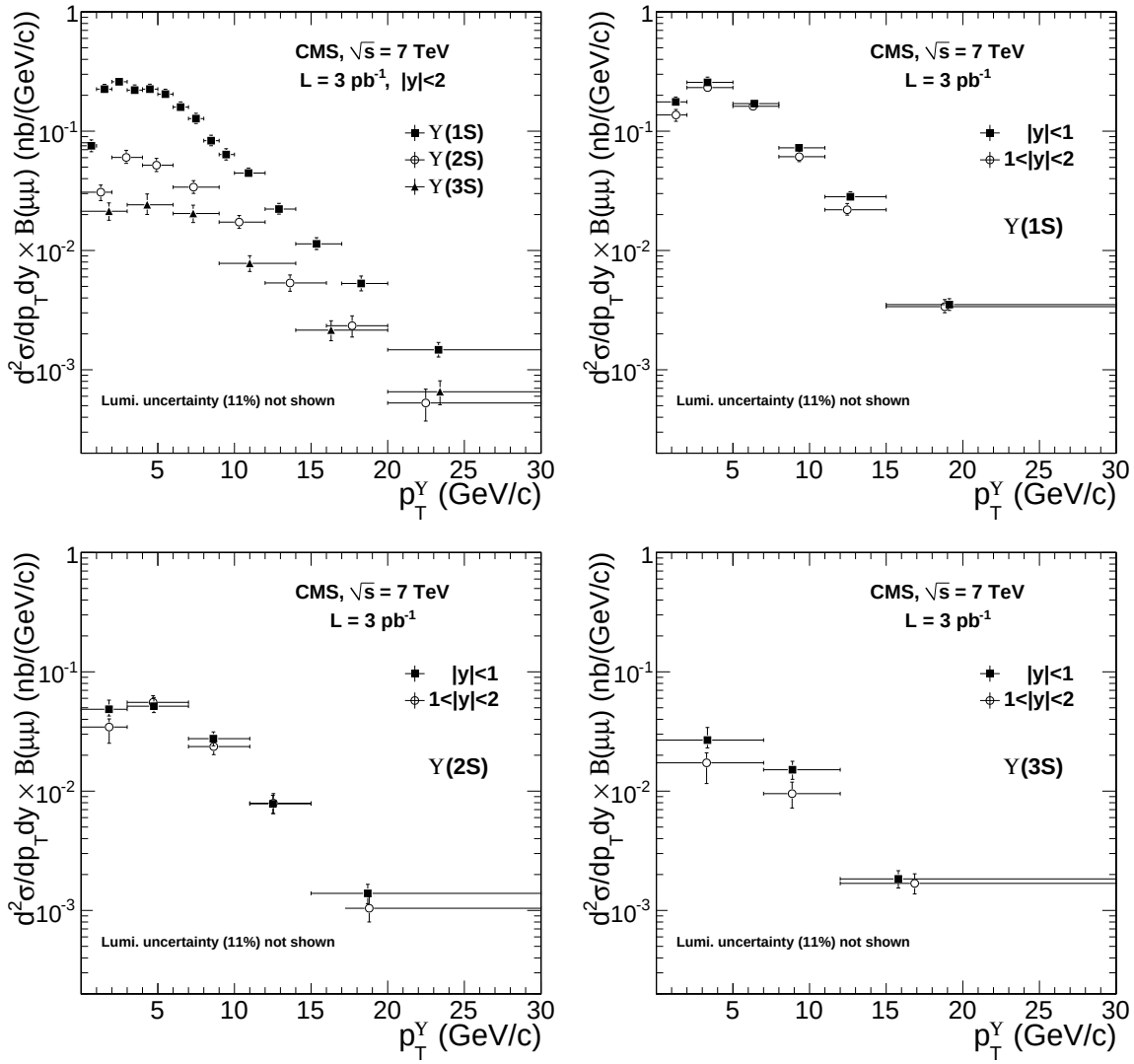

Figure 6: $\Upsilon(nS)$ differential cross sections in the rapidity interval $|y| < 2$ (top left), and in the rapidity intervals $|y| < 1$ and $1 < |y| < 2$ for the $\Upsilon(1\mathrm{S})$ (top right), $\Upsilon(2\mathrm{S})$ (botttom left) and $\Upsilon(3\mathrm{S})$ (bottom right). The uncertainties on the points represent the sum of the statistical and systematic uncertainties added in quadrature, excluding the uncertainty on the integrated luminosity (11%).

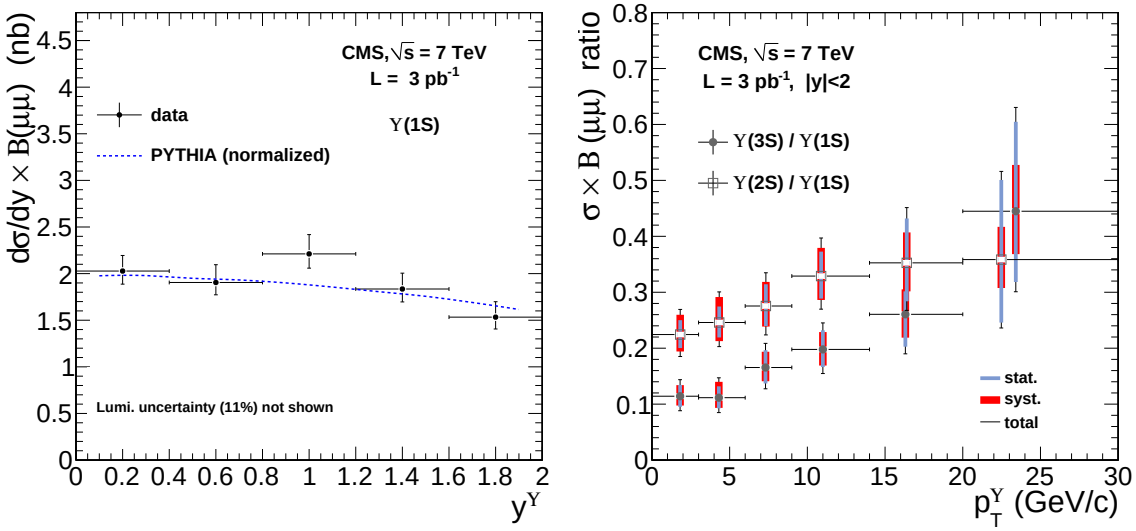

Figure 7: (Left) $\Upsilon(1S)$ rapidity-differential cross section in the transverse momentum range $p_T < 30\,\text{GeV}/c$ (data points) and normalized PYTHIA prediction (line). The uncertainties on the points represent the sum of the statistical and systematic uncertainties added in quadrature, excluding the uncertainty on the integrated luminosity (11%). (Right) $\Upsilon(nS)$ cross-section ratios as a function of p_T in the rapidity range $|y| < 2$.

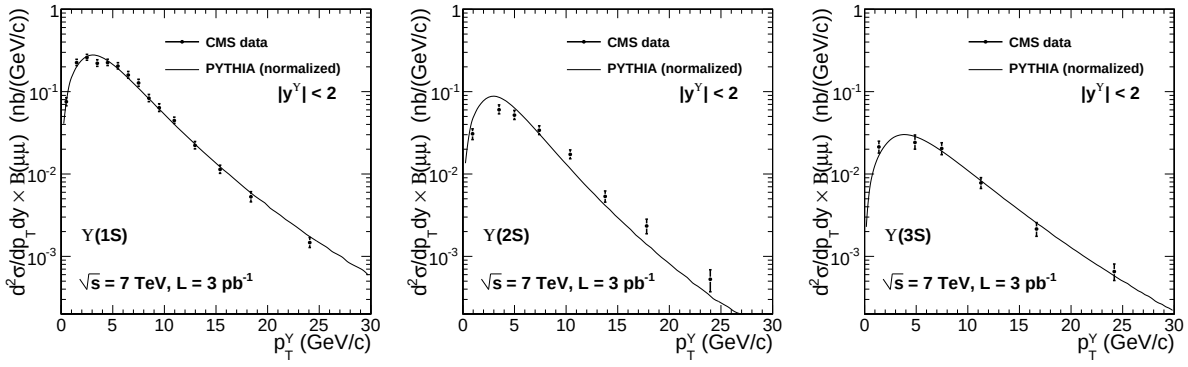

Figure 8: Differential cross sections of the $\Upsilon(nS)$ as a function of p_T in the rapidity range $|y| < 2$, and comparison to the PYTHIA predictions normalized to the measured p_T-integrated cross sections; $\Upsilon(1S)$ (left), $\Upsilon(2S)$ (middle), and $\Upsilon(3S)$ (right). The PYTHIA curve is used to calculate the abscissa of the data points [28]. The uncertainties on the points represent the sum of the statistical and systematic uncertainties added in quadrature, excluding the uncertainty on the integrated luminosity (11%).

The $\Upsilon(nS)$ integrated cross sections are expected to increase with $\sqrt{s}$. We compare our measurement of the $\Upsilon(1S)$ integrated cross section in the central rapidity region $|y| < 1$ to previous measurements from the DØ and CDF experiments [4, 5] in Table 11. Previous measurements are restricted to the range $p_T < 20\,\text{GeV}/c$ and $|y| < 0.4$ for CDF and $|y| < 1.8$ for DØ. Under the assumption that the cross section is uniform in rapidity for the measurement range of each experiment, the cross section we measure at $\sqrt{s} = 7\,\text{TeV}$ is about three times larger than the cross section measured at the Tevatron. Although our measurement extends to higher p_T than the Tevatron measurements, the fraction of the cross section satisfying $p_T > 20\,\text{GeV}/c$ is less than 1% and so can be neglected for this comparison. We compare the normalized p_T-differential cross sections at the Tevatron to our measurements in Fig. 9.

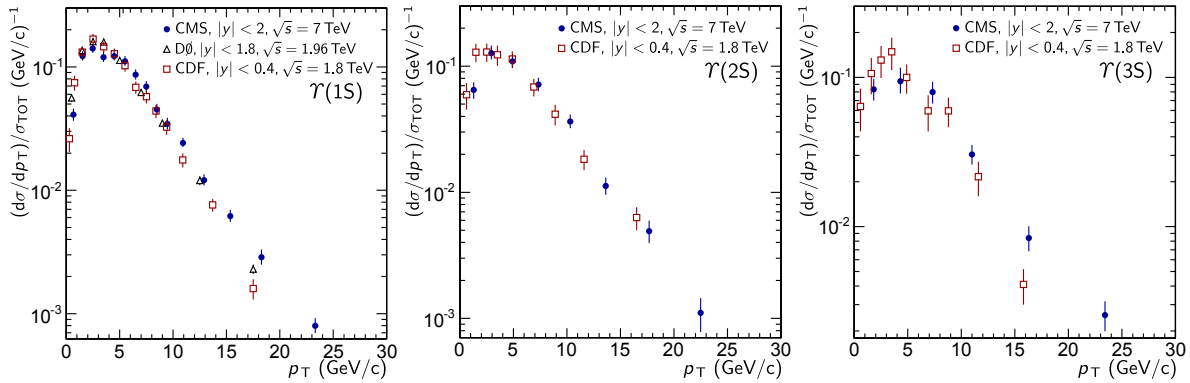

Figure 9: Comparison of the CMS differential $\Upsilon(nS)$ cross sections as a function of p_T, normalized by $\sigma_{TOT} = \sum(d\sigma/dp_T)\Delta p_T$, to previous measurements; $\Upsilon(1S)$ (left), $\Upsilon(2S)$ (middle), and $\Upsilon(3S)$ (right).

9 Summary

The study of the $\Upsilon(nS)$ resonances provides important information on the process of hadroproduction of heavy quarks. In this paper we have presented the first measurement of the $\Upsilon(nS)$ differential production cross section for proton-proton collisions at $\sqrt{s} = 7\,\text{TeV}$. Integrated over the range $p_T < 30\,\text{GeV}/c$ and $|y| < 2$, we find the product of the $\Upsilon(1S)$ production cross section and dimuon branching fraction to be $\sigma(\text{pp} \to \Upsilon(1S)X) \cdot \mathcal{B}(\Upsilon(1S) \to \mu^+\mu^-) = 7.37 \pm 0.13^{+0.61}_{-0.42} \pm 0.81\,\text{nb}$, where the first uncertainty is statistical, the second is systematic, and the third is associated with the estimation of the integrated luminosity of the data sample. Under the assumption that the cross section is uniform in rapidity for the measurement range of each experiment, the cross section we measure at $\sqrt{s} = 7\,\text{TeV}$ is about three times larger than the cross section measured at the Tevatron. The $\Upsilon(2S)$ and $\Upsilon(3S)$ integrated cross sections and the $\Upsilon(1S)$, $\Upsilon(2S)$, and $\Upsilon(3S)$ differential cross sections in transverse momentum in two regions of rapidity have also been determined. The differential cross-section measurements have been compared to previous measurements and PYTHIA. Finally, the cross section ratios of the three $\Upsilon(nS)$ have been measured.

The dominant sources of systematic uncertainty on the cross-section measurement arise from the tag-and-probe determination of the efficiencies and from the integrated luminosity normalization. Both will be reduced with additional data. The cross sections obtained in this work assume unpolarized $\Upsilon(nS)$ production. Assuming fully-transverse or fully-longitudinal polarization changes the cross section by about 20%. With a larger accumulated data sample, it will become possible to perform a simultaneous measurement of the polarization and the cross section. This work provides new experimental results which will serve as input to ongoing

theoretical investigations of the correct description of bottomonium production.

Acknowledgments
We wish to congratulate our colleagues in the CERN accelerator departments for the excellent performance of the LHC machine. We thank the technical and administrative staff at CERN and other CMS institutes. This work was supported by the Austrian Federal Ministry of Science and Research; the Belgium Fonds de la Recherche Scientifique, and Fonds voor Wetenschappelijk Onderzoek; the Brazilian Funding Agencies (CNPq, CAPES, FAPERJ, and FAPESP); the Bulgarian Ministry of Education and Science; CERN; the Chinese Academy of Sciences, Ministry of Science and Technology, and National Natural Science Foundation of China; the Colombian Funding Agency (COLCIENCIAS); the Croatian Ministry of Science, Education and Sport; the Research Promotion Foundation, Cyprus; the Estonian Academy of Sciences and NICPB; the Academy of Finland, Finnish Ministry of Education, and Helsinki Institute of Physics; the Institut National de Physique Nucléaire et de Physique des Particules / CNRS, and Commissariat à l'Énergie Atomique, France; the Bundesministerium für Bildung und Forschung, Deutsche Forschungsgemeinschaft, and Helmholtz-Gemeinschaft Deutscher Forschungszentren, Germany; the General Secretariat for Research and Technology, Greece; the National Scientific Research Foundation, and National Office for Research and Technology, Hungary; the Department of Atomic Energy, and Department of Science and Technology, India; the Institute for Studies in Theoretical Physics and Mathematics, Iran; the Science Foundation, Ireland; the Istituto Nazionale di Fisica Nucleare, Italy; the Korean Ministry of Education, Science and Technology and the World Class University program of NRF, Korea; the Lithuanian Academy of Sciences; the Mexican Funding Agencies (CINVESTAV, CONACYT, SEP, and UASLP-FAI); the Pakistan Atomic Energy Commission; the State Commission for Scientific Research, Poland; the Fundação para a Ciência e a Tecnologia, Portugal; JINR (Armenia, Belarus, Georgia, Ukraine, Uzbekistan); the Ministry of Science and Technologies of the Russian Federation, and Russian Ministry of Atomic Energy; the Ministry of Science and Technological Development of Serbia; the Ministerio de Ciencia e Innovación, and Programa Consolider-Ingenio 2010, Spain; the Swiss Funding Agencies (ETH Board, ETH Zurich, PSI, SNF, UniZH, Canton Zurich, and SER); the National Science Council, Taipei; the Scientific and Technical Research Council of Turkey, and Turkish Atomic Energy Authority; the Science and Technology Facilities Council, UK; the US Department of Energy, and the US National Science Foundation. Individuals have received support from the Marie-Curie IEF program (European Union); the Leventis Foundation; the A. P. Sloan Foundation; the Alexander von Humboldt Foundation; the Associazione per lo Sviluppo Scientifico e Tecnologico del Piemonte (Italy); the Belgian Federal Science Policy Office; the Fonds pour la Formation à la Recherche dans l'índustrie et dans l'Ágriculture (FRIA-Belgium); and the Agentschap voor Innovatie door Wetenschap en Technologie (IWT-Belgium).

References

[1] N. Brambilla et al., "Heavy quarkonium physics", *CERN-2005-005* (2004).

[2] G. T. Bodwin, E. Braaten, and G. P. Lepage, "Rigorous QCD analysis of inclusive annihilation and production of heavy quarkonium", *Phys. Rev.* **D51** (1995) 1125. doi:10.1103/PhysRevD.51.1125.

[3] P. Artoisenet et al., "Y production at Fermilab Tevatron and LHC energies", *Phys. Rev. Lett.* **101** (2008) 152001. doi:10.1103/PhysRevLett.101.152001.

[4] CDF Collaboration, "Upsilon production and polarization in $p\bar{p}$ collisions at $\sqrt{s} =$ 1.8-TeV", *Phys. Rev. Lett.* **88** (2002) 161802. doi:10.1103/PhysRevLett.88.161802.

[5] D0 Collaboration, "Measurement of inclusive differential cross sections for Υ(1S) production in $p\bar{p}$ collisions at $\sqrt{s}$ = 1.96-TeV", *Phys. Rev. Lett.* **94** (2005) 232001, arXiv:hep-ex/0502030. And *Erratum, Phys. Rev. Lett.* **100** (2008) 049902. doi:10.1103/PhysRevLett.100.049902.

[6] T. Sjöstrand, S. Mrenna, and P. Z. Skands, "PYTHIA 6.4 physics and manual", *JHEP* **0605** (2006) 026. doi:10.1088/1126-6708/2006/05/026.

[7] CMS Collaboration, "The CMS experiment at the CERN LHC", *JINST* **0803** (2008) S08004. doi:10.1088/1748-0221/3/08/S08004.

[8] CMS Collaboration, "Measurement of CMS Luminosity", *CMS Physics Analysis Summary* **CMS-PAS-EWK-10-004** (2010).

[9] CMS Collaboration, "CMS Tracking Performance Results from early LHC Operation", *Eur. Phys. J.* **C70** (2010) 1165, arXiv:1007.1988. doi:10.1140/epjc/s10052-010-1491-3.

[10] CMS Collaboration, "Alignment of the CMS silicon tracker during commissioning with cosmic rays", *JINST* **5** (2010) T03009. doi:10.1088/1748-0221/5/03/T03009.

[11] M. Krämer, "Quarkonium production at high-energy colliders", *Prog. Part. Nucl. Phys.* **47** (2001) 141. doi:10.1016/S0146-6410(01)00154-5.

[12] M. Bargiotti and V. Vagnoni, "Heavy quarkonia sector in PYTHIA 6.324: tuning, validation and perspectives at LHC", *LHCb-2007-042* (2007).

[13] E. Barberio, B. van Eijk, and Z. Wąs, "PHOTOS - a universal Monte Carlo for QED radiative corrections in decays", *Comput. Phys. Commun.* **66** (1991) 115. doi:10.1016/0010-4655(91)90012-A.

[14] E. Barberio and Z. Was, "PHOTOS - a universal Monte Carlo for QED radiative corrections: version 2.0", *Comput. Phys. Commun.* **79** (1994) 291. doi:10.1016/0010-4655(94)90074-4.

[15] S. Agostinelli et al., "G4 - a simulation toolkit", *Nucl. Instrum. Meth.* **A506** (2003) 250. doi:10.1016/S0168-9002(03)01368-8.

[16] CMS Collaboration, "Performance of muon identification in pp collisions at $\sqrt{s}$ = 7 TeV", *CMS Physics Analysis Summary* **CMS-PAS-MUO-10-002** (2010).

[17] CMS Collaboration, "Precise mapping of the magnetic field in the CMS barrel yoke using cosmic rays", *JINST* **5** (2010) T03021. doi:10.1088/1748-0221/5/03/T03021.

[18] CMS Collaboration, "Studies of Tracker Material in the CMS Detector", *CMS Physics Analysis Summary* **CMS-PAS-TRK-10-003** (2010).

[19] CMS Collaboration, "Measurement of Momentum Scale and Resolution using Low-mass Resonances and Cosmic Ray Muons", *CMS Physics Analysis Summary* **CMS-PAS-TRK-10-004** (2010).

[20] D. J. Lange, "The EvtGen particle decay simulation package", *Nucl. Instrum. Meth.* **A462** (2001) 152. doi:10.1016/S0168-9002(01)00089-4.

[21] P. Faccioli et al., "Towards the experimental clarification of quarkonium polarization", *Eur. Phys. J.* **C69** (2010) 657. doi:10.1140/epjc/s10052-010-1420-5.

[22] J. C. Collins and D. E. Soper, "Angular Distribution of Dileptons in High-Energy Hadron Collisions", *Phys. Rev.* **D16** (1977) 2219. doi:10.1103/PhysRevD.16.2219.

[23] CMS Collaboration, "Measurement of tracking efficiency", *CMS Physics Analysis Summary* **CMS-PAS-TRK-10-002** (2010).

[24] CMS Collaboration, "Prompt and non-prompt J/psi production in pp collisions at sqrt(s) = 7 TeV", *submitted to Eur. Phys. J.* (2010) arXiv:1011.4193.

[25] M. J. Oreglia, "A Study of the Reactions psi prime → gamma gamma psi", *Ph.D. Thesis* **SLAC-R-236** (1980) Appendix D.

[26] Particle Data Group Collaboration, "Review of particle physics", *J. Phys.* **G37** (2010) 075021. doi:10.1088/0954-3899/37/7A/075021.

[27] CMS Collaboration, "Performance of CMS Muon Reconstruction in Cosmic-Ray Events", *JINST* **5** (2010) T03022, arXiv:0911.4994. doi:10.1088/1748-0221/5/03/T03022.

[28] G. D. Lafferty and T. R. Wyatt, "Where to stick your data points: the treatment of measurements within wide bins", *Nucl. Instrum. Meth.* **A355** (1995) 541. doi:10.1016/0168-9002(94)01112-5.

Table 3: The uncorrected Υ signal yield, fit quality (normalized χ^2, obtained by comparing the fit PDF and the binned data; the number of degrees of freedom is 112), and average weight $\langle w \rangle$ in p_T intervals for $|y| < 2$. The mean of the p_T distribution in each interval is also given.

	p_T (GeV/c)		fit	signal	
	range	mean	χ^2	yield	$\langle w \rangle^{-1}$
Υ(1S)	0–1	0.7	1.1	427±34	0.44
	1–2	1.5	1.7	1153±54	0.41
	2–3	2.5	1.1	1154±53	0.36
	3–4	3.5	1.3	806±46	0.30
	4–5	4.5	1.0	769±43	0.28
	5–6	5.5	1.1	716±40	0.28
	6–7	6.5	1.2	578±37	0.28
	7–8	7.5	1.3	477±33	0.30
	8–9	8.5	1.1	344±26	0.34
	9–10	9.5	1.1	286±24	0.37
	10–12	10.9	1.1	449±27	0.41
	12–14	12.9	1.3	246±19	0.45
	14–17	15.4	1.2	208±18	0.50
	17–20	18.3	0.8	105±13	0.54
	20–30	23.3	0.8	109±13	0.60
	sum			7825±133	
	combined fit			7807±133	
Υ(2S)	0–2	1.3	1.7	368±41	0.47
	2–4	2.9	1.3	591±50	0.40
	4–6	4.9	0.9	416±40	0.32
	6–9	7.3	1.1	424±38	0.33
	9–12	10.3	1.1	257±25	0.41
	12–16	13.6	1.3	121±16	0.46
	16–20	17.7	1.0	63±11	0.55
	20–30	22.5	0.8	39±9	0.60
	sum			2279±91	
	combined fit			2270±91	
Υ(3S)	0–3	1.8	1.5	397±51	0.47
	3–6	4.3	1.0	326±47	0.37
	6–9	7.3	1.1	264±36	0.35
	9–14	11.0	1.2	207±25	0.43
	14–20	16.3	1.2	83±14	0.52
	20–30	23.4	0.8	49±10	0.61
	sum			1324±84	
	combined fit			1318±84	

Table 4: The product of the $\Upsilon(nS)$ production cross sections, σ, and the dimuon branching fraction, $\mathcal{B}$, measured in p_T bins for $|y| < 2$, with the assumption of unpolarized production. The statistical uncertainty (stat.), the sum of the systematic uncertainties in quadrature ($\Sigma_{\text{syst.}}$), and the total uncertainty ($\Delta\sigma$; including stat., $\Sigma_{\text{syst.}}$, and luminosity terms) are quoted as relative uncertainties in percent. Values in parentheses denote the negative part of the asymmetric uncertainty. The fractional change in percent of the cross section is shown for four polarization scenarios: fully-longitudinal (L) and fully-transverse (T) in the helicity (HX) and Collins-Soper (CS) frames.

p_T (GeV/c)	$\sigma \cdot \mathcal{B}$ (nb)	stat. (%)	$\Sigma_{\text{syst.}}$ (%)	$\Delta\sigma$ (%)	HX-T (%)	HX-L (%)	CS-T (%)	CS-L (%)
		$\Upsilon(1S)$		$\lvert y\rvert < 2$				
0–30	7.37	1.8	8 (6)	14 (13)	+16	-22	+13	-16
0– 1	0.30	8	10 (7)	17 (15)	+16	-22	+17	-23
1– 2	0.90	5	9 (6)	15 (14)	+16	-20	+19	-24
2– 3	1.04	5	8 (6)	14 (13)	+15	-20	+19	-24
3–4	0.88	6	9 (7)	15 (14)	+18	-23	+18	-23
4–5	0.90	6	8 (6)	15 (14)	+18	-23	+16	-21
5–6	0.82	6	8 (6)	15 (14)	+17	-23	+13	-19
6–7	0.64	7	8 (5)	15 (14)	+17	-22	+11	-16
7–8	0.51	7	8 (6)	15 (14)	+16	-22	+7	-10
8–9	0.33	8	8 (6)	16 (14)	+16	-22	+4	-5
9–10	0.25	8	9 (6)	16 (15)	+15	-21	+2	-1
10–12	0.36	6	8 (5)	15 (14)	+15	-21	-1	+3
12–14	0.18	8	9 (5)	16 (14)	+15	-20	-3	+7
14–17	0.14	9	10 (6)	17 (15)	+14	-19	-4	+9
17–20	0.06	12	10 (6)	19 (17)	+13	-18	-4	+10
20–30	0.06	12	10 (6)	19 (17)	+12	-17	-4	+10
		$\Upsilon(2S)$		$\lvert y\rvert < 2$				
0–30	1.90	4.2	9 (6)	15 (13)	+14	-19	+12	-15
0–2	0.25	12	11 (9)	20 (19)	+14	-19	+17	-22
2–4	0.48	8	12 (10)	18 (17)	+12	-17	+18	-23
4–6	0.41	10	10 (8)	18 (17)	+16	-22	+15	-20
6–9	0.41	9	10 (7)	17 (16)	+15	-21	+9	-13
9–12	0.21	10	9 (6)	17 (16)	+14	-20	+1	-0
12–16	0.09	13	10 (7)	20 (19)	+14	-19	-2	+6
16–20	0.04	18	11 (8)	24 (23)	+12	-18	-4	+9
20–30	0.02	23	20 (18)	32 (32)	+12	-17	-5	+11
		$\Upsilon(3S)$		$\lvert y\rvert < 2$				
0–30	1.02	6.7	11 (8)	17 (15)	+14	-19	+10	-13
0–3	0.26	14	10 (8)	21 (19)	+13	-18	+16	-22
3–6	0.29	14	18 (17)	26 (25)	+13	-18	+16	-21
6–9	0.24	14	11 (8)	21 (19)	+15	-20	+10	-13
9–14	0.16	12	10 (8)	19 (18)	+15	-20	-1	+2
14–20	0.05	17	11 (8)	23 (22)	+13	-18	-4	+9
20–30	0.03	20	12 (9)	26 (25)	+11	-16	-4	+9

Table 5: The product of the $\Upsilon(nS)$ production cross sections, σ, and the dimuon branching fraction, $\mathcal{B}$, measured in p_T bins for $|y| < 1$ and $1 < |y| < 2$, with the assumption of unpolarized production. The statistical uncertainty (stat.), the sum of the systematic uncertainties in quadrature ($\Sigma_{\text{syst.}}$), and the total uncertainty ($\Delta\sigma$; including stat., $\sum_{\text{syst.}}$, and luminosity terms) are quoted as relative uncertainties in percent. Values in parentheses denote the negative part of the asymmetric uncertainty. The fractional change in percent of the cross section is shown for four polarization scenarios: fully-longitudinal (L) and fully-transverse (T) in the helicity (HX) and Collins-Soper (CS) frames.

p_T (GeV/c)	$\sigma \cdot \mathcal{B}$ (nb)	stat. (%)	$\sum_{\text{syst.}}$ (%)	$\Delta\sigma$ (%)	HX-T (%)	HX-L (%)	CS-T (%)	CS-L (%)
		$\Upsilon(1S)$		$\lvert y\rvert < 1$				
0–30	4.03	1.3	8 (6)	14 (12)	+16	-22	+13	-16
0–2	0.70	5	9 (7)	15 (14)	+14	-19	+18	-24
2–5	1.54	4	10 (9)	15 (15)	+14	-20	+18	-23
5–8	1.02	5	7 (6)	14 (13)	+18	-23	+8	-12
8–11	0.44	6	7 (5)	15 (14)	+18	-23	-1	+2
11–15	0.23	7	8 (5)	15 (14)	+18	-23	-4	+10
15–30	0.11	9	8 (6)	16 (15)	+15	-20	-5	+12
		$\Upsilon(2S)$		$\lvert y\rvert < 1$				
0–30	1.03	2.9	9 (6)	15 (13)	+14	-19	+12	-15
0–3	0.29	10	17 (16)	22 (21)	+10	-14	+17	-22
3–7	0.41	10	16 (15)	21 (21)	+13	-18	+14	-19
7–11	0.22	11	9 (7)	18 (17)	+17	-22	+1	-2
11–15	0.06	16	9 (6)	21 (20)	+17	-22	-4	+8
15–30	0.04	17	9 (7)	22 (21)	+14	-20	-5	+11
		$\Upsilon(3S)$		$\lvert y\rvert < 1$				
0–30	0.59	4.8	11 (8)	16 (15)	+14	-19	+10	-13
0–7	0.38	11	25 (24)	30 (29)	+11	-16	+14	-19
7–12	0.15	15	10 (8)	21 (20)	+16	-22	+1	-1
12–30	0.07	14	10 (8)	20 (20)	+15	-21	-4	+10
		$\Upsilon(1S)$		$1 < \lvert y\rvert < 2$				
0–30	3.55	1.2	8 (6)	14 (12)	+16	-22	+13	-16
0–2	0.55	7	11 (9)	17 (16)	+18	-24	+18	-23
2–5	1.39	4	9 (7)	15 (14)	+20	-25	+18	-23
5–8	0.97	5	9 (5)	15 (13)	+16	-22	+14	-18
8–11	0.37	7	10 (6)	16 (14)	+13	-19	+6	-8
11–15	0.18	8	10 (6)	17 (15)	+11	-17	0	+1
15–30	0.10	9	11 (6)	18 (16)	+10	-16	-3	+6
		$\Upsilon(2S)$		$1 < \lvert y\rvert < 2$				
0–30	0.93	3.0	9 (6)	15 (13)	+14	-19	+12	-15
0–3	0.21	15	24 (23)	30 (29)	+17	-23	+17	-23
3–7	0.44	9	12 (8)	18 (17)	+17	-22	+17	-22
7–11	0.19	12	11 (8)	20 (18)	+13	-18	+9	-12
11–15	0.06	17	11 (7)	23 (21)	+11	-17	+1	0
15–30	0.03	21	13 (9)	27 (26)	+10	-16	-3	+7
		$\Upsilon(3S)$		$1 < \lvert y\rvert < 2$				
0–30	0.40	4.9	11 (8)	16 (15)	+14	-19	+10	-13
0–7	0.24	18	29 (27)	36 (35)	+16	-22	+17	-22
7–12	0.10	22	13 (10)	28 (27)	+13	-18	+10	-13
12–30	0.06	17	11 (8)	23 (22)	+10	-15	-2	+5

Table 6: The product of the $\Upsilon(1S)$ production cross section, σ, and the dimuon branching fraction, $\mathcal{B}$, measured in rapidity bins and integrated over the p_T range $p_T^\Upsilon < 30\,\mathrm{GeV}/c$, with the assumption of unpolarized production. The statistical uncertainty (stat.), the sum of the systematic uncertainties in quadrature ($\Sigma_{\mathrm{syst.}}$), and the total uncertainty ($\Delta\sigma$; including stat., $\sum_{\mathrm{syst.}}$, and luminosity terms) are quoted as relative uncertainties in percent. Values in parentheses denote the negative part of the asymmetric uncertainty. The fractional change in percent of the cross section is shown for four polarization scenarios: fully-longitudinal (L) and fully-transverse (T) in the helicity (HX) and Collins-Soper (CS) frames.

$\lvert y\rvert$	$\sigma\cdot\mathcal{B}$ (nb)	stat. (%)	$\sum_{\mathrm{syst.}}$ (%)	$\Delta\sigma$ (%)	HX-T (%)	HX-L (%)	CS-T (%)	CS-L (%)
		$\Upsilon(1S)$		$p_T < 30\,\mathrm{GeV}/c$				
0.0–2.0	7.61	1.8	8 (6)	14 (13)	+16	-22	+13	-16
0.0–0.4	1.62	3	8 (6)	14 (13)	+15	-19	+13	-17
0.4–0.8	1.52	4	9 (8)	15 (14)	+17	-22	+11	-15
0.8–1.2	1.77	4	9 (7)	14 (13)	+16	-22	+9	-12
1.2–1.6	1.47	4	9 (7)	15 (13)	+17	-23	+12	-16
1.6–2.0	1.23	4	11 (7)	16 (14)	+18	-23	+20	-24

Table 7: Relative values of the systematic uncertainties on the $\Upsilon(nS)$ production cross sections times the dimuon branching fraction, in p_T intervals for $|y| < 2$, assuming unpolarized production, in percent. The following abbreviations are used: A, $\varepsilon_{\text{trig,id}}$, S_p, A_{p_T}, A_{vtx}, A_{FSR}, T&P, and $\varepsilon_{J/\psi,\Upsilon}$, for the systematic uncertainties arising from imperfect knowledge of the acceptance, trigger and muon identification efficiencies, momentum scale, the production p_T spectrum, the efficiency of the vertex quality criterion, the modeling of FSR, the T&P method, and the bias from using the J/ψ to determine single-muon efficiencies rather than the Υ. The uncertainties associated with the background PDF are in the column labeled BG, while the signal PDF, the fitter, tracking efficiency, and effects arising from the efficiency binning are combined in the column labeled add. Values in parentheses denote the negative part of the asymmetric uncertainty. The luminosity uncertainty of 11% is not included in the table.

p_T (GeV/c)	A	$\varepsilon_{\text{trig,id}}$	S_p	A_{p_T}	A_{vtx}	A_{FSR}	T&P	$\varepsilon_{J/\psi,\Upsilon}$	BG	add.
	Υ(1S)	$\|y\| < 2$	uncertainties are in percent							
0–30	0.5 (0.5)	7.5 (4.6)	0.3 (0.3)	0.6	0.7	0.7	0.0	0.9	0.5	3.0
0–1	0.4 (0.4)	8.3 (5.4)	0.1 (0.1)	0.2	1.1	0.8	0.5	0.8	3.4	3.1
1–2	0.4 (0.4)	7.8 (5.2)	0.2 (0.2)	0.6	0.6	0.7	0.2	1.1	1.8	3.0
2–3	0.5 (0.5)	7.3 (4.7)	0.6 (0.6)	0.3	0.3	0.8	0.1	1.1	1.5	3.0
3–4	0.6 (0.6)	7.3 (4.8)	0.6 (0.6)	0.1	0.4	0.8	0.0	1.1	3.7	3.0
4–5	0.6 (0.6)	7.4 (4.5)	0.4 (0.3)	0.3	0.7	0.7	0.0	0.9	2.3	3.0
5–6	0.6 (0.6)	7.4 (4.3)	0.2 (0.3)	0.5	1.0	0.7	0.0	0.7	0.5	3.0
6–7	0.6 (0.6)	7.4 (4.1)	0.2 (0.3)	0.7	1.1	0.6	0.1	0.7	0.4	3.0
7–8	0.6 (0.6)	7.7 (4.7)	0.1 (0.1)	1.0	0.7	0.6	0.2	0.8	1.0	3.1
8–9	0.6 (0.6)	7.4 (4.2)	0.0 (0.1)	1.2	0.7	0.5	0.0	0.7	1.0	3.0
9–10	0.5 (0.5)	7.8 (4.3)	0.1 (0.0)	1.3	0.9	0.5	0.2	0.6	1.9	3.1
10–12	0.5 (0.5)	7.4 (3.7)	0.1 (0.1)	1.4	0.8	0.5	0.2	0.6	0.2	3.0
12–14	0.5 (0.4)	7.9 (4.0)	0.2 (0.1)	1.6	0.9	0.5	0.1	0.6	0.3	3.1
14–17	0.4 (0.4)	8.5 (4.2)	0.1 (0.1)	1.6	0.9	0.5	0.3	0.6	2.2	3.1
17–20	0.4 (0.4)	8.9 (4.4)	0.1 (0.1)	1.8	0.8	0.4	0.5	0.7	0.1	3.6
20–30	0.3 (0.3)	8.9 (4.3)	0.1 (0.1)	1.6	0.7	0.5	0.3	0.6	0.1	3.5
	Υ(2S)	$\|y\| < 2$								
0–30	0.6 (0.6)	8.3 (4.9)	0.3 (0.3)	0.7	0.8	0.8	0.0	1.0	1.9	3.2
0–2	0.5 (0.5)	8.3 (5.2)	0.2 (0.2)	0.5	0.6	0.8	0.4	0.6	6.8	3.3
2–4	0.7 (0.7)	8.3 (5.4)	0.7 (0.8)	0.2	0.3	1.0	0.1	1.5	8.0	3.3
4–6	0.8 (0.7)	7.9 (4.7)	0.4 (0.4)	0.4	1.1	0.8	0.0	0.9	5.2	3.3
6–9	0.7 (0.7)	8.6 (4.8)	0.1 (0.1)	1.0	1.2	0.7	0.2	0.9	1.7	3.5
9–12	0.5 (0.5)	8.4 (4.2)	0.1 (0.1)	1.5	1.0	0.5	0.2	0.8	0.9	3.6
12–16	0.4 (0.5)	8.8 (4.6)	0.1 (0.1)	1.6	0.9	0.5	0.3	0.8	2.0	4.0
16–20	0.3 (0.4)	8.3 (4.1)	0.2 (0.1)	1.7	1.0	0.5	0.4	0.5	0.0	6.5
20–30	0.3 (0.3)	9.1 (4.4)	0.1 (0.1)	1.7	0.8	0.5	0.2	0.3	0.0	17.3
	Υ(3S)	$\|y\| < 2$								
0–30	0.7 (0.6)	8.6 (4.7)	0.3 (0.3)	0.8	0.8	0.8	0.1	1.0	3.4	5.4
0–3	0.5 (0.5)	8.5 (4.4)	0.4 (0.5)	0.5	0.4	0.9	0.2	0.6	1.7	5.7
3–6	0.9 (0.8)	9.1 (5.4)	0.7 (0.7)	0.3	0.9	1.0	0.0	1.7	14.1	7.3
6–9	0.7 (0.7)	8.9 (4.8)	0.2 (0.2)	1.1	1.0	0.7	0.0	1.0	2.2	5.6
9–14	0.5 (0.5)	7.5 (4.1)	0.1 (0.1)	1.5	0.8	0.5	0.3	0.7	0.4	6.1
14–20	0.4 (0.4)	8.8 (4.5)	0.2 (0.1)	1.7	0.8	0.5	0.3	0.6	3.4	5.9
20–30	0.3 (0.3)	8.8 (4.1)	0.1 (0.1)	1.6	0.8	0.5	0.5	0.5	0.3	8.3

Table 8: Relative values of the systematic uncertainties on the $\Upsilon(nS)$ production cross sections times the dimuon branching fraction, in p_T intervals for $|y| < 1$ and $1 < |y| < 2$, assuming unpolarized production, in percent. The following abbreviations are used: A, $\varepsilon_{\text{trig,id}}$, S_p, A_{p_T}, A_{vtx}, A_{FSR}, T&P, and $\varepsilon_{J/\psi,\Upsilon}$, for the systematic uncertainties arising from imperfect knowledge of the acceptance, trigger and muon identification efficiencies, momentum scale, the production p_T spectrum, the efficiency of the vertex quality criterion, the modeling of FSR, the T&P method, and the bias from using the J/ψ to determine single-muon efficiencies rather than the Υ. The uncertainties associated with the background PDF are in the column labeled BG, while the signal PDF, the fitter, tracking efficiency, and effects arising from the efficiency binning are combined in the column labeled add. Values in parentheses denote the negative part of the asymmetric uncertainty. The luminosity uncertainty of 11% is not included in the table.

p_T (GeV/c)	A	$\varepsilon_{\text{trig,id}}$	S_p	A_{p_T}	A_{vtx}	A_{FSR}	T&P	$\varepsilon_{J/\psi,\Upsilon}$	BG	add.
	Υ(1S)	$\|y\| < 1$	uncertainties are in percent							
0-30	0.5 (0.5)	7.5 (4.6)	0.3 (0.3)	0.6	0.7	0.7	0.0	0.9	0.5	3.0
0-2	0.4 (0.4)	7.7 (5.6)	0.3 (0.3)	0.6	0.5	0.7	0.7	1.3	1.6	3.0
2-5	0.6 (0.6)	7.1 (5.2)	0.7 (0.7)	0.2	0.1	0.9	0.3	1.5	6.2	3.0
5-8	0.7 (0.7)	6.5 (4.4)	0.3 (0.3)	0.8	0.8	0.7	0.4	1.0	0.3	3.0
8-11	0.5 (0.5)	6.4 (3.9)	0.0 (0.0)	1.3	0.5	0.5	0.3	0.7	0.6	3.0
11-15	0.5 (0.4)	6.6 (3.8)	0.1 (0.1)	1.5	0.7	0.5	0.3	0.6	0.4	3.0
15-30	0.3 (0.4)	7.1 (4.2)	0.1 (0.2)	1.6	0.6	0.5	0.3	0.5	0.9	3.0
	Υ(2S)	$\|y\| < 1$								
0-30	0.6 (0.6)	8.3 (4.9)	0.3 (0.3)	0.7	0.8	0.8	0.0	1.0	1.9	3.2
0-3	0.6 (0.5)	8.2 (6.0)	0.6 (0.6)	0.5	0.1	1.0	0.7	1.4	13.9	3.4
3-7	0.8 (0.8)	7.7 (5.2)	0.6 (0.7)	0.4	0.6	1.0	0.4	1.5	13.1	3.4
7-11	0.6 (0.6)	7.7 (4.9)	0.1 (0.0)	1.3	0.8	0.6	0.3	1.0	1.7	3.4
11-15	0.5 (0.5)	7.3 (4.4)	0.1 (0.1)	1.6	0.8	0.5	0.3	0.7	1.6	3.6
15-30	0.3 (0.4)	7.4 (4.3)	0.1 (0.2)	1.7	0.5	0.5	0.2	0.4	1.9	4.2
	Υ(3S)	$\|y\| < 1$								
0-30	0.7 (0.6)	8.6 (4.7)	0.3 (0.3)	0.8	0.8	0.8	0.1	1.0	3.4	5.4
0-7	0.8 (0.8)	8.8 (5.9)	0.6 (0.7)	0.5	0.5	1.0	0.5	1.7	22.9	5.4
7-12	0.6 (0.6)	7.6 (5.0)	0.0 (0.0)	1.4	0.6	0.6	0.1	0.9	2.2	5.7
12-30	0.4 (0.4)	7.1 (4.0)	0.2 (0.1)	1.6	0.7	0.5	0.3	0.5	0.2	6.0
	Υ(1S)	$1 < \|y\| < 2$								
0-30	0.5 (0.5)	7.5 (4.6)	0.3 (0.3)	0.6	0.7	0.7	0.0	0.9	0.5	3.0
0-2	0.4 (0.4)	8.2 (4.6)	0.0 (0.1)	0.3	1.1	0.6	0.2	0.6	7.3	3.0
2-5	0.5 (0.5)	7.7 (4.0)	0.3 (0.3)	0.2	0.9	0.7	0.3	0.5	4.3	3.0
5-8	0.6 (0.6)	8.4 (4.2)	0.1 (0.2)	0.7	1.2	0.6	0.5	0.6	0.4	3.0
8-11	0.6 (0.5)	8.9 (4.4)	0.0 (0.1)	1.3	1.1	0.5	0.6	0.7	1.7	3.1
11-15	0.4 (0.5)	9.1 (4.2)	0.1 (0.2)	1.6	0.9	0.5	0.8	0.6	0.1	3.0
15-30	0.4 (0.5)	10.6 (4.3)	0.2 (0.3)	1.7	1.1	0.5	0.9	0.8	2.0	3.1
	Υ(2S)	$1 < \|y\| < 2$								
0-30	0.6 (0.6)	8.3 (4.9)	0.3 (0.3)	0.7	0.8	0.8	0.0	1.0	1.9	3.3
0-3	0.5 (0.5)	7.8 (3.8)	0.2 (0.2)	0.3	1.2	0.7	0.2	0.5	21.9	3.8
3-7	0.7 (0.7)	9.4 (4.9)	0.3 (0.3)	0.4	1.3	0.8	0.4	0.6	5.4	3.4
7-11	0.6 (0.6)	9.6 (4.8)	0.0 (0.0)	1.2	1.1	0.6	0.7	0.8	4.4	3.5
11-15	0.5 (0.5)	9.7 (4.8)	0.1 (0.2)	1.6	0.9	0.5	1.1	0.7	1.5	4.6
15-30	0.4 (0.4)	9.5 (3.8)	0.2 (0.2)	1.7	1.3	0.4	1.0	0.7	3.4	7.2
	Υ(3S)	$1 < \|y\| < 2$								
0-30	0.7 (0.6)	8.6 (4.7)	0.3 (0.3)	0.8	0.8	0.8	0.1	1.0	3.4	5.5
0-7	0.7 (0.6)	8.6 (2.9)	0.4 (0.4)	0.4	1.1	0.8	0.5	0.3	26.5	6.5
7-12	0.7 (0.6)	9.3 (4.1)	0.0 (0.0)	1.3	1.0	0.6	1.1	0.6	6.2	6.7
12-30	0.4 (0.4)	9.4 (4.3)	0.1 (0.2)	1.7	1.1	0.5	0.9	0.5	1.5	5.9

Table 9: Relative values of the systematic uncertainties on the Υ(1S) production cross section times the dimuon branching fraction, in rapidity intervals for $p_T < 30\,\text{GeV}/c$, assuming unpolarized production, in percent. The following abbreviations are used: A, $\varepsilon_{\text{trig,id}}$, S_p, A_{p_T}, A_{vtx}, A_{FSR}, T&P, and $\varepsilon_{J/\psi,\Upsilon}$, for the systematic uncertainties arising from imperfect knowledge of the acceptance, trigger and muon identification efficiencies, momentum scale, the production p_T spectrum, the efficiency of the vertex quality criterion, the modeling of FSR, the T&P method, and the bias from using the J/ψ to determine single-muon efficiencies rather than the Υ. The uncertainties associated with the background PDF are in the column labeled BG, while the signal PDF, the fitter, tracking efficiency, and effects arising from the efficiency binning are combined in the column labeled add. Values in parentheses denote the negative part of the asymmetric uncertainty. The luminosity uncertainty of 11% is not included in the table.

$\lvert y\rvert$	A	$\varepsilon_{\text{trig,id}}$	S_p	A_{p_T}	A_{vtx}	A_{FSR}	t&p	$\varepsilon_{J/\psi,\Upsilon}$	BG	add.
Υ(1S) $p_T < 30\,\text{GeV}/c$ uncertainties are in percent										
0.0-2.0	0.5	7.5 (4.6)	0.3 (0.3)	0.6	0.7	0.7	0.0	0.9	0.5	3.0
0.0-0.4	0.6	6.8 (4.9)	0.4 (0.4)	0.7	0.3	0.7	0.6	1.5	0.1	3.0
0.4-0.8	0.6	6.8 (4.7)	0.4 (0.4)	0.6	0.3	0.7	0.3	1.1	5.4	3.0
0.8-1.2	0.5	7.5 (4.9)	0.3 (0.3)	0.6	1.0	0.7	0.1	0.7	2.9	3.0
1.2-1.6	0.5	7.7 (4.0)	0.2 (0.2)	0.6	1.2	0.6	0.2	0.5	4.0	3.0
1.6-2.0	0.6	9.3 (4.0)	0.0 (0.1)	0.6	0.9	0.6	0.9	0.6	5.0	3.0

Table 10: The ratios of $\Upsilon(nS)$ cross sections for different Υ p_T ranges in the unpolarized scenario. The first uncertainty is statistical and the second is systematic. The ratios are independent of the luminosity normalization and its uncertainty.

p_T (GeV/c)	Υ(3S) / Υ(1S)	Υ(2S) / Υ(1S)
0–30	$0.14 \pm 0.01 \pm 0.02$	$0.26 \pm 0.02 \pm 0.04$
0–3	$0.11 \pm 0.02 \pm 0.02$	$0.22 \pm 0.03 \pm 0.04$
3–6	$0.11 \pm 0.02 \pm 0.03$	$0.25 \pm 0.03 \pm 0.05$
6–9	$0.17 \pm 0.03 \pm 0.03$	$0.28 \pm 0.04 \pm 0.04$
9–14	$0.20 \pm 0.03 \pm 0.03$	$0.33 \pm 0.04 \pm 0.05$
14–20	$0.26 \pm 0.07 \pm 0.04$	$0.35 \pm 0.08 \pm 0.05$
20–30	$0.44 \pm 0.16 \pm 0.08$	$0.36 \pm 0.14 \pm 0.06$

Table 11: Υ(1S) cross-section measurements at several center-of-mass collision energies. The first uncertainty is statistical, the second is systematic, and the third is associated with the luminosity determination.

Exp.	$\sqrt{s}$ (TeV)	$\frac{d\sigma}{dy}(p\bar{p} \to \Upsilon(1S)X) \cdot B(\Upsilon \to \mu\mu)$	rapidity range
CDF	1.8	$0.680 \pm 0.015 \pm 0.018 \pm 0.026$ nb [4]	$\lvert y\rvert < 0.4$
DØ	1.96	$0.628 \pm 0.016 \pm 0.065 \pm 0.038$ nb [5]	$\lvert y\rvert < 0.6$
CMS	7.0	$2.02 \pm 0.03^{+0.16}_{-0.12} \pm 0.22$ nb (this work)	$\lvert y\rvert < 1.0$

A The CMS Collaboration

Yerevan Physics Institute, Yerevan, Armenia
V. Khachatryan, A.M. Sirunyan, A. Tumasyan

Institut für Hochenergiephysik der OeAW, Wien, Austria
W. Adam, T. Bergauer, M. Dragicevic, J. Erö, C. Fabjan, M. Friedl, R. Frühwirth, V.M. Ghete, J. Hammer[1], S. Hänsel, C. Hartl, M. Hoch, N. Hörmann, J. Hrubec, M. Jeitler, G. Kasieczka, W. Kiesenhofer, M. Krammer, D. Liko, I. Mikulec, M. Pernicka, H. Rohringer, R. Schöfbeck, J. Strauss, A. Taurok, F. Teischinger, W. Waltenberger, G. Walzel, E. Widl, C.-E. Wulz

National Centre for Particle and High Energy Physics, Minsk, Belarus
V. Mossolov, N. Shumeiko, J. Suarez Gonzalez

Universiteit Antwerpen, Antwerpen, Belgium
L. Benucci, L. Ceard, K. Cerny, E.A. De Wolf, X. Janssen, T. Maes, L. Mucibello, S. Ochesanu, B. Roland, R. Rougny, M. Selvaggi, H. Van Haevermaet, P. Van Mechelen, N. Van Remortel

Vrije Universiteit Brussel, Brussel, Belgium
V. Adler, S. Beauceron, F. Blekman, S. Blyweert, J. D'Hondt, O. Devroede, R. Gonzalez Suarez, A. Kalogeropoulos, J. Maes, M. Maes, S. Tavernier, W. Van Doninck, P. Van Mulders, G.P. Van Onsem, I. Villella

Université Libre de Bruxelles, Bruxelles, Belgium
O. Charaf, B. Clerbaux, G. De Lentdecker, V. Dero, A.P.R. Gay, G.H. Hammad, T. Hreus, P.E. Marage, L. Thomas, C. Vander Velde, P. Vanlaer, J. Wickens

Ghent University, Ghent, Belgium
S. Costantini, M. Grunewald, B. Klein, A. Marinov, J. Mccartin, D. Ryckbosch, F. Thyssen, M. Tytgat, L. Vanelderen, P. Verwilligen, S. Walsh, N. Zaganidis

Université Catholique de Louvain, Louvain-la-Neuve, Belgium
S. Basegmez, G. Bruno, J. Caudron, J. De Favereau De Jeneret, C. Delaere, P. Demin, D. Favart, A. Giammanco, G. Grégoire, J. Hollar, V. Lemaitre, J. Liao, O. Militaru, S. Ovyn, D. Pagano, A. Pin, K. Piotrzkowski, L. Quertenmont, N. Schul

Université de Mons, Mons, Belgium
N. Beliy, T. Caebergs, E. Daubie

Centro Brasileiro de Pesquisas Fisicas, Rio de Janeiro, Brazil
G.A. Alves, D. De Jesus Damiao, M.E. Pol, M.H.G. Souza

Universidade do Estado do Rio de Janeiro, Rio de Janeiro, Brazil
W. Carvalho, E.M. Da Costa, C. De Oliveira Martins, S. Fonseca De Souza, L. Mundim, H. Nogima, V. Oguri, W.L. Prado Da Silva, A. Santoro, S.M. Silva Do Amaral, A. Sznajder

Instituto de Fisica Teorica, Universidade Estadual Paulista, Sao Paulo, Brazil
F.A. Dias, M.A.F. Dias, T.R. Fernandez Perez Tomei, E. M. Gregores[2], F. Marinho, S.F. Novaes, Sandra S. Padula

Institute for Nuclear Research and Nuclear Energy, Sofia, Bulgaria
N. Darmenov[1], L. Dimitrov, V. Genchev[1], P. Iaydjiev[1], S. Piperov, M. Rodozov, S. Stoykova, G. Sultanov, V. Tcholakov, R. Trayanov, I. Vankov

University of Sofia, Sofia, Bulgaria
M. Dyulendarova, R. Hadjiiska, V. Kozhuharov, L. Litov, E. Marinova, M. Mateev, B. Pavlov, P. Petkov

Institute of High Energy Physics, Beijing, China
J.G. Bian, G.M. Chen, H.S. Chen, C.H. Jiang, D. Liang, S. Liang, J. Wang, J. Wang, X. Wang, Z. Wang, M. Xu, M. Yang, J. Zang, Z. Zhang

State Key Lab. of Nucl. Phys. and Tech., Peking University, Beijing, China
Y. Ban, S. Guo, W. Li, Y. Mao, S.J. Qian, H. Teng, L. Zhang, B. Zhu

Universidad de Los Andes, Bogota, Colombia
A. Cabrera, B. Gomez Moreno, A.A. Ocampo Rios, A.F. Osorio Oliveros, J.C. Sanabria

Technical University of Split, Split, Croatia
N. Godinovic, D. Lelas, K. Lelas, R. Plestina[3], D. Polic, I. Puljak

University of Split, Split, Croatia
Z. Antunovic, M. Dzelalija

Institute Rudjer Boskovic, Zagreb, Croatia
V. Brigljevic, S. Duric, K. Kadija, S. Morovic

University of Cyprus, Nicosia, Cyprus
A. Attikis, M. Galanti, J. Mousa, C. Nicolaou, F. Ptochos, P.A. Razis, H. Rykaczewski

Academy of Scientific Research and Technology of the Arab Republic of Egypt, Egyptian Network of High Energy Physics, Cairo, Egypt
Y. Assran[4], M.A. Mahmoud[5]

National Institute of Chemical Physics and Biophysics, Tallinn, Estonia
A. Hektor, M. Kadastik, K. Kannike, M. Müntel, M. Raidal, L. Rebane

Department of Physics, University of Helsinki, Helsinki, Finland
V. Azzolini, P. Eerola

Helsinki Institute of Physics, Helsinki, Finland
S. Czellar, J. Härkönen, A. Heikkinen, V. Karimäki, R. Kinnunen, J. Klem, M.J. Kortelainen, T. Lampén, K. Lassila-Perini, S. Lehti, T. Lindén, P. Luukka, T. Mäenpää, E. Tuominen, J. Tuominiemi, E. Tuovinen, D. Ungaro, L. Wendland

Lappeenranta University of Technology, Lappeenranta, Finland
K. Banzuzi, A. Korpela, T. Tuuva

Laboratoire d'Annecy-le-Vieux de Physique des Particules, IN2P3-CNRS, Annecy-le-Vieux, France
D. Sillou

DSM/IRFU, CEA/Saclay, Gif-sur-Yvette, France
M. Besancon, S. Choudhury, M. Dejardin, D. Denegri, B. Fabbro, J.L. Faure, F. Ferri, S. Ganjour, F.X. Gentit, A. Givernaud, P. Gras, G. Hamel de Monchenault, P. Jarry, E. Locci, J. Malcles, M. Marionneau, L. Millischer, J. Rander, A. Rosowsky, I. Shreyber, M. Titov, P. Verrecchia

Laboratoire Leprince-Ringuet, Ecole Polytechnique, IN2P3-CNRS, Palaiseau, France
S. Baffioni, F. Beaudette, L. Bianchini, M. Bluj[6], C. Broutin, P. Busson, C. Charlot, T. Dahms, L. Dobrzynski, R. Granier de Cassagnac, M. Haguenauer, P. Miné, C. Mironov, C. Ochando, P. Paganini, D. Sabes, R. Salerno, Y. Sirois, C. Thiebaux, B. Wyslouch[7], A. Zabi

Institut Pluridisciplinaire Hubert Curien, Université de Strasbourg, Université de Haute Alsace Mulhouse, CNRS/IN2P3, Strasbourg, France
J.-L. Agram[8], J. Andrea, A. Besson, D. Bloch, D. Bodin, J.-M. Brom, M. Cardaci, E.C. Chabert, C. Collard, E. Conte[8], F. Drouhin[8], C. Ferro, J.-C. Fontaine[8], D. Gelé, U. Goerlach, S. Greder, P. Juillot, M. Karim[8], A.-C. Le Bihan, Y. Mikami, P. Van Hove

Centre de Calcul de l'Institut National de Physique Nucleaire et de Physique des Particules (IN2P3), Villeurbanne, France
F. Fassi, D. Mercier

Université de Lyon, Université Claude Bernard Lyon 1, CNRS-IN2P3, Institut de Physique Nucléaire de Lyon, Villeurbanne, France
C. Baty, N. Beaupere, M. Bedjidian, O. Bondu, G. Boudoul, D. Boumediene, H. Brun, N. Chanon, R. Chierici, D. Contardo, P. Depasse, H. El Mamouni, A. Falkiewicz, J. Fay, S. Gascon, B. Ille, T. Kurca, T. Le Grand, M. Lethuillier, L. Mirabito, S. Perries, V. Sordini, S. Tosi, Y. Tschudi, P. Verdier, H. Xiao

E. Andronikashvili Institute of Physics, Academy of Science, Tbilisi, Georgia
V. Roinishvili

RWTH Aachen University, I. Physikalisches Institut, Aachen, Germany
G. Anagnostou, M. Edelhoff, L. Feld, N. Heracleous, O. Hindrichs, R. Jussen, K. Klein, J. Merz, N. Mohr, A. Ostapchuk, A. Perieanu, F. Raupach, J. Sammet, S. Schael, D. Sprenger, H. Weber, M. Weber, B. Wittmer

RWTH Aachen University, III. Physikalisches Institut A, Aachen, Germany
M. Ata, W. Bender, M. Erdmann, J. Frangenheim, T. Hebbeker, A. Hinzmann, K. Hoepfner, C. Hof, T. Klimkovich, D. Klingebiel, P. Kreuzer, D. Lanske†, C. Magass, G. Masetti, M. Merschmeyer, A. Meyer, P. Papacz, H. Pieta, H. Reithler, S.A. Schmitz, L. Sonnenschein, J. Steggemann, D. Teyssier

RWTH Aachen University, III. Physikalisches Institut B, Aachen, Germany
M. Bontenackels, M. Davids, M. Duda, G. Flügge, H. Geenen, M. Giffels, W. Haj Ahmad, D. Heydhausen, T. Kress, Y. Kuessel, A. Linn, A. Nowack, L. Perchalla, O. Pooth, J. Rennefeld, P. Sauerland, A. Stahl, M. Thomas, D. Tornier, M.H. Zoeller

Deutsches Elektronen-Synchrotron, Hamburg, Germany
M. Aldaya Martin, W. Behrenhoff, U. Behrens, M. Bergholz[9], K. Borras, A. Cakir, A. Campbell, E. Castro, D. Dammann, G. Eckerlin, D. Eckstein, A. Flossdorf, G. Flucke, A. Geiser, I. Glushkov, J. Hauk, H. Jung, M. Kasemann, I. Katkov, P. Katsas, C. Kleinwort, H. Kluge, A. Knutsson, D. Krücker, E. Kuznetsova, W. Lange, W. Lohmann[9], R. Mankel, M. Marienfeld, I.-A. Melzer-Pellmann, A.B. Meyer, J. Mnich, A. Mussgiller, J. Olzem, A. Parenti, A. Raspereza, A. Raval, R. Schmidt[9], T. Schoerner-Sadenius, N. Sen, M. Stein, J. Tomaszewska, D. Volyanskyy, R. Walsh, C. Wissing

University of Hamburg, Hamburg, Germany
C. Autermann, S. Bobrovskyi, J. Draeger, H. Enderle, U. Gebbert, K. Kaschube, G. Kaussen, R. Klanner, J. Lange, B. Mura, S. Naumann-Emme, F. Nowak, N. Pietsch, C. Sander, H. Schettler, P. Schleper, M. Schröder, T. Schum, J. Schwandt, A.K. Srivastava, H. Stadie, G. Steinbrück, J. Thomsen, R. Wolf

Institut für Experimentelle Kernphysik, Karlsruhe, Germany
C. Barth, J. Bauer, V. Buege, T. Chwalek, W. De Boer, A. Dierlamm, G. Dirkes, M. Feindt, J. Gruschke, C. Hackstein, F. Hartmann, S.M. Heindl, M. Heinrich, H. Held, K.H. Hoffmann,

S. Honc, T. Kuhr, D. Martschei, S. Mueller, Th. Müller, M. Niegel, O. Oberst, A. Oehler, J. Ott, T. Peiffer, D. Piparo, G. Quast, K. Rabbertz, F. Ratnikov, M. Renz, C. Saout, A. Scheurer, P. Schieferdecker, F.-P. Schilling, G. Schott, H.J. Simonis, F.M. Stober, D. Troendle, J. Wagner-Kuhr, M. Zeise, V. Zhukov[10], E.B. Ziebarth

Institute of Nuclear Physics "Demokritos", Aghia Paraskevi, Greece
G. Daskalakis, T. Geralis, S. Kesisoglou, A. Kyriakis, D. Loukas, I. Manolakos, A. Markou, C. Markou, C. Mavrommatis, E. Petrakou

University of Athens, Athens, Greece
L. Gouskos, T.J. Mertzimekis, A. Panagiotou[1]

University of Ioánnina, Ioánnina, Greece
I. Evangelou, C. Foudas, P. Kokkas, N. Manthos, I. Papadopoulos, V. Patras, F.A. Triantis

KFKI Research Institute for Particle and Nuclear Physics, Budapest, Hungary
A. Aranyi, G. Bencze, L. Boldizsar, G. Debreczeni, C. Hajdu[1], D. Horvath[11], A. Kapusi, K. Krajczar[12], A. Laszlo, F. Sikler, G. Vesztergombi[12]

Institute of Nuclear Research ATOMKI, Debrecen, Hungary
N. Beni, J. Molnar, J. Palinkas, Z. Szillasi, V. Veszpremi

University of Debrecen, Debrecen, Hungary
P. Raics, Z.L. Trocsanyi, B. Ujvari

Panjab University, Chandigarh, India
S. Bansal, S.B. Beri, V. Bhatnagar, N. Dhingra, M. Jindal, M. Kaur, J.M. Kohli, M.Z. Mehta, N. Nishu, L.K. Saini, A. Sharma, A.P. Singh, J.B. Singh, S.P. Singh

University of Delhi, Delhi, India
S. Ahuja, S. Bhattacharya, B.C. Choudhary, P. Gupta, S. Jain, S. Jain, A. Kumar, R.K. Shivpuri

Bhabha Atomic Research Centre, Mumbai, India
R.K. Choudhury, D. Dutta, S. Kailas, S.K. Kataria, A.K. Mohanty[1], L.M. Pant, P. Shukla, P. Suggisetti

Tata Institute of Fundamental Research - EHEP, Mumbai, India
T. Aziz, M. Guchait[13], A. Gurtu, M. Maity[14], D. Majumder, G. Majumder, K. Mazumdar, G.B. Mohanty, A. Saha, K. Sudhakar, N. Wickramage

Tata Institute of Fundamental Research - HECR, Mumbai, India
S. Banerjee, S. Dugad, N.K. Mondal

Institute for Studies in Theoretical Physics & Mathematics (IPM), Tehran, Iran
H. Arfaei, H. Bakhshiansohi, S.M. Etesami, A. Fahim, M. Hashemi, A. Jafari, M. Khakzad, A. Mohammadi, M. Mohammadi Najafabadi, S. Paktinat Mehdiabadi, B. Safarzadeh, M. Zeinali

INFN Sezione di Bari [a], Università di Bari [b], Politecnico di Bari [c], Bari, Italy
M. Abbrescia[a,b], L. Barbone[a,b], C. Calabria[a,b], A. Colaleo[a], D. Creanza[a,c], N. De Filippis[a,c], M. De Palma[a,b], A. Dimitrov[a], L. Fiore[a], G. Iaselli[a,c], L. Lusito[a,b,1], G. Maggi[a,c], M. Maggi[a], N. Manna[a,b], B. Marangelli[a,b], S. My[a,c], S. Nuzzo[a,b], N. Pacifico[a,b], G.A. Pierro[a], A. Pompili[a,b], G. Pugliese[a,c], F. Romano[a,c], G. Roselli[a,b], G. Selvaggi[a,b], L. Silvestris[a], R. Trentadue[a], S. Tupputi[a,b], G. Zito[a]

INFN Sezione di Bologna [a], Università di Bologna [b], Bologna, Italy
G. Abbiendi[a], A.C. Benvenuti[a], D. Bonacorsi[a], S. Braibant-Giacomelli[a,b], P. Capiluppi[a,b], A. Castro[a,b], F.R. Cavallo[a], M. Cuffiani[a,b], G.M. Dallavalle[a], F. Fabbri[a], A. Fanfani[a,b], D. Fasanella[a], P. Giacomelli[a], M. Giunta[a], C. Grandi[a], S. Marcellini[a], M. Meneghelli[a,b], A. Montanari[a], F.L. Navarria[a,b], F. Odorici[a], A. Perrotta[a], F. Primavera[a], A.M. Rossi[a,b], T. Rovelli[a,b], G. Siroli[a,b], R. Travaglini[a,b]

INFN Sezione di Catania [a], Università di Catania [b], Catania, Italy
S. Albergo[a,b], G. Cappello[a,b], M. Chiorboli[a,b,1], S. Costa[a,b], A. Tricomi[a,b], C. Tuve[a]

INFN Sezione di Firenze [a], Università di Firenze [b], Firenze, Italy
G. Barbagli[a], V. Ciulli[a,b], C. Civinini[a], R. D'Alessandro[a,b], E. Focardi[a,b], S. Frosali[a,b], E. Gallo[a], C. Genta[a], P. Lenzi[a,b], M. Meschini[a], S. Paoletti[a], G. Sguazzoni[a], A. Tropiano[a,1]

INFN Laboratori Nazionali di Frascati, Frascati, Italy
L. Benussi, S. Bianco, S. Colafranceschi[15], F. Fabbri, D. Piccolo

INFN Sezione di Genova, Genova, Italy
P. Fabbricatore, R. Musenich

INFN Sezione di Milano-Biccoca [a], Università di Milano-Bicocca [b], Milano, Italy
A. Benaglia[a,b], F. De Guio[a,b,1], L. Di Matteo[a,b], A. Ghezzi[a,b,1], M. Malberti[a,b], S. Malvezzi[a], A. Martelli[a,b], A. Massironi[a,b], D. Menasce[a], L. Moroni[a], M. Paganoni[a,b], D. Pedrini[a], S. Ragazzi[a,b], N. Redaelli[a], S. Sala[a], T. Tabarelli de Fatis[a,b], V. Tancini[a,b]

INFN Sezione di Napoli [a], Università di Napoli "Federico II" [b], Napoli, Italy
S. Buontempo[a], C.A. Carrillo Montoya[a], A. Cimmino[a,b], A. De Cosa[a,b], M. De Gruttola[a,b], F. Fabozzi[a,16], A.O.M. Iorio[a], L. Lista[a], M. Merola[a,b], P. Noli[a,b], P. Paolucci[a]

INFN Sezione di Padova [a], Università di Padova [b], Università di Trento (Trento) [c], Padova, Italy
P. Azzi[a], N. Bacchetta[a], P. Bellan[a,b], D. Bisello[a,b], A. Branca[a], R. Carlin[a,b], P. Checchia[a], M. De Mattia[a,b], T. Dorigo[a], U. Dosselli[a], F. Fanzago[a], F. Gasparini[a,b], U. Gasparini[a,b], P. Giubilato[a,b], A. Gresele[a,c], S. Lacaprara[a,17], I. Lazzizzera[a,c], M. Margoni[a,b], M. Mazzucato[a], A.T. Meneguzzo[a,b], M. Nespolo[a], L. Perrozzi[a,1], N. Pozzobon[a,b], P. Ronchese[a,b], F. Simonetto[a,b], E. Torassa[a], M. Tosi[a,b], S. Vanini[a,b], P. Zotto[a,b], G. Zumerle[a,b]

INFN Sezione di Pavia [a], Università di Pavia [b], Pavia, Italy
P. Baesso[a,b], U. Berzano[a], C. Riccardi[a,b], P. Torre[a,b], P. Vitulo[a,b], C. Viviani[a,b]

INFN Sezione di Perugia [a], Università di Perugia [b], Perugia, Italy
M. Biasini[a,b], G.M. Bilei[a], B. Caponeri[a,b], L. Fanò[a,b], P. Lariccia[a,b], A. Lucaroni[a,b,1], G. Mantovani[a,b], M. Menichelli[a], A. Nappi[a,b], A. Santocchia[a,b], L. Servoli[a], S. Taroni[a,b], M. Valdata[a,b], R. Volpe[a,b,1]

INFN Sezione di Pisa [a], Università di Pisa [b], Scuola Normale Superiore di Pisa [c], Pisa, Italy
P. Azzurri[a,c], G. Bagliesi[a], J. Bernardini[a,b], T. Boccali[a,1], G. Broccolo[a,c], R. Castaldi[a], R.T. D'Agnolo[a,c], R. Dell'Orso[a], F. Fiori[a,b], L. Foà[a,c], A. Giassi[a], A. Kraan[a], F. Ligabue[a,c], T. Lomtadze[a], L. Martini[a], A. Messineo[a,b], F. Palla[a], F. Palmonari[a], S. Sarkar[a,c], A.T. Serban[a], P. Spagnolo[a], R. Tenchini[a], G. Tonelli[a,b,1], A. Venturi[a,1], P.G. Verdini[a]

INFN Sezione di Roma [a], Università di Roma "La Sapienza" [b], Roma, Italy
L. Barone[a,b], F. Cavallari[a], D. Del Re[a,b], E. Di Marco[a,b], M. Diemoz[a], D. Franci[a,b], M. Grassi[a], E. Longo[a,b], G. Organtini[a,b], A. Palma[a,b], F. Pandolfi[a,b,1], R. Paramatti[a], S. Rahatlou[a,b]

INFN Sezione di Torino [a], Università di Torino [b], Università del Piemonte Orientale (Novara) [c], Torino, Italy
N. Amapane[a,b], R. Arcidiacono[a,c], S. Argiro[a,b], M. Arneodo[a,c], C. Biino[a], C. Botta[a,b,1], N. Cartiglia[a], R. Castello[a,b], M. Costa[a,b], N. Demaria[a], A. Graziano[a,b,1], C. Mariotti[a], M. Marone[a,b], S. Maselli[a], E. Migliore[a,b], G. Mila[a,b], V. Monaco[a,b], M. Musich[a,b], M.M. Obertino[a,c], N. Pastrone[a], M. Pelliccioni[a,b,1], A. Romero[a,b], M. Ruspa[a,c], R. Sacchi[a,b], V. Sola[a,b], A. Solano[a,b], A. Staiano[a], D. Trocino[a,b], A. Vilela Pereira[a,b,1]

INFN Sezione di Trieste [a], Università di Trieste [b], Trieste, Italy
F. Ambroglini[a,b], S. Belforte[a], F. Cossutti[a], G. Della Ricca[a,b], B. Gobbo[a], D. Montanino[a,b], A. Penzo[a]

Kangwon National University, Chunchon, Korea
S.G. Heo

Kyungpook National University, Daegu, Korea
S. Chang, J. Chung, D.H. Kim, G.N. Kim, J.E. Kim, D.J. Kong, H. Park, D. Son, D.C. Son

Chonnam National University, Institute for Universe and Elementary Particles, Kwangju, Korea
Zero Kim, J.Y. Kim, S. Song

Korea University, Seoul, Korea
S. Choi, B. Hong, M. Jo, H. Kim, J.H. Kim, T.J. Kim, K.S. Lee, D.H. Moon, S.K. Park, H.B. Rhee, E. Seo, S. Shin, K.S. Sim

University of Seoul, Seoul, Korea
M. Choi, S. Kang, H. Kim, C. Park, I.C. Park, S. Park, G. Ryu

Sungkyunkwan University, Suwon, Korea
Y. Choi, Y.K. Choi, J. Goh, J. Lee, S. Lee, H. Seo, I. Yu

Vilnius University, Vilnius, Lithuania
M.J. Bilinskas, I. Grigelionis, M. Janulis, D. Martisiute, P. Petrov, T. Sabonis

Centro de Investigacion y de Estudios Avanzados del IPN, Mexico City, Mexico
H. Castilla Valdez, E. De La Cruz Burelo, R. Lopez-Fernandez, A. Sánchez Hernández, L.M. Villasenor-Cendejas

Universidad Iberoamericana, Mexico City, Mexico
S. Carrillo Moreno, F. Vazquez Valencia

Benemerita Universidad Autonoma de Puebla, Puebla, Mexico
H.A. Salazar Ibarguen

Universidad Autónoma de San Luis Potosí, San Luis Potosí, Mexico
E. Casimiro Linares, A. Morelos Pineda, M.A. Reyes-Santos

University of Auckland, Auckland, New Zealand
P. Allfrey, D. Krofcheck

University of Canterbury, Christchurch, New Zealand
P.H. Butler, R. Doesburg, H. Silverwood

National Centre for Physics, Quaid-I-Azam University, Islamabad, Pakistan
M. Ahmad, I. Ahmed, M.I. Asghar, H.R. Hoorani, W.A. Khan, T. Khurshid, S. Qazi

Institute of Experimental Physics, Faculty of Physics, University of Warsaw, Warsaw, Poland
M. Cwiok, W. Dominik, K. Doroba, A. Kalinowski, M. Konecki, J. Krolikowski

Soltan Institute for Nuclear Studies, Warsaw, Poland
T. Frueboes, R. Gokieli, M. Górski, M. Kazana, K. Nawrocki, K. Romanowska-Rybinska, M. Szleper, G. Wrochna, P. Zalewski

Laboratório de Instrumentação e Física Experimental de Partículas, Lisboa, Portugal
N. Almeida, A. David, P. Faccioli, P.G. Ferreira Parracho, M. Gallinaro, P. Martins, P. Musella, A. Nayak, P.Q. Ribeiro, J. Seixas, P. Silva, J. Varela[1], H.K. Wöhri

Joint Institute for Nuclear Research, Dubna, Russia
I. Belotelov, P. Bunin, M. Finger, M. Finger Jr., I. Golutvin, A. Kamenev, V. Karjavin, G. Kozlov, A. Lanev, P. Moisenz, V. Palichik, V. Perelygin, S. Shmatov, V. Smirnov, A. Volodko, A. Zarubin

Petersburg Nuclear Physics Institute, Gatchina (St Petersburg), Russia
N. Bondar, V. Golovtsov, Y. Ivanov, V. Kim, P. Levchenko, V. Murzin, V. Oreshkin, I. Smirnov, V. Sulimov, L. Uvarov, S. Vavilov, A. Vorobyev

Institute for Nuclear Research, Moscow, Russia
Yu. Andreev, S. Gninenko, N. Golubev, M. Kirsanov, N. Krasnikov, V. Matveev, A. Pashenkov, A. Toropin, S. Troitsky

Institute for Theoretical and Experimental Physics, Moscow, Russia
V. Epshteyn, V. Gavrilov, V. Kaftanov†, M. Kossov[1], A. Krokhotin, N. Lychkovskaya, G. Safronov, S. Semenov, V. Stolin, E. Vlasov, A. Zhokin

Moscow State University, Moscow, Russia
E. Boos, M. Dubinin[18], L. Dudko, A. Ershov, A. Gribushin, O. Kodolova, I. Lokhtin, S. Obraztsov, S. Petrushanko, L. Sarycheva, V. Savrin, A. Snigirev

P.N. Lebedev Physical Institute, Moscow, Russia
V. Andreev, M. Azarkin, I. Dremin, M. Kirakosyan, S.V. Rusakov, A. Vinogradov

State Research Center of Russian Federation, Institute for High Energy Physics, Protvino, Russia
I. Azhgirey, S. Bitioukov, V. Grishin[1], V. Kachanov, D. Konstantinov, A. Korablev, V. Krychkine, V. Petrov, R. Ryutin, S. Slabospitsky, A. Sobol, L. Tourtchanovitch, S. Troshin, N. Tyurin, A. Uzunian, A. Volkov

University of Belgrade, Faculty of Physics and Vinca Institute of Nuclear Sciences, Belgrade, Serbia
P. Adzic[19], M. Djordjevic, D. Krpic[19], J. Milosevic

Centro de Investigaciones Energéticas Medioambientales y Tecnológicas (CIEMAT), Madrid, Spain
M. Aguilar-Benitez, J. Alcaraz Maestre, P. Arce, C. Battilana, E. Calvo, M. Cepeda, M. Cerrada, N. Colino, B. De La Cruz, C. Diez Pardos, D. Domínguez Vázquez, C. Fernandez Bedoya, J.P. Fernández Ramos, A. Ferrando, J. Flix, M.C. Fouz, P. Garcia-Abia, O. Gonzalez Lopez, S. Goy Lopez, J.M. Hernandez, M.I. Josa, G. Merino, J. Puerta Pelayo, I. Redondo, L. Romero, J. Santaolalla, C. Willmott

Universidad Autónoma de Madrid, Madrid, Spain
C. Albajar, G. Codispoti, J.F. de Trocóniz

Universidad de Oviedo, Oviedo, Spain
J. Cuevas, J. Fernandez Menendez, S. Folgueras, I. Gonzalez Caballero, L. Lloret Iglesias, J.M. Vizan Garcia

Instituto de Física de Cantabria (IFCA), CSIC-Universidad de Cantabria, Santander, Spain
J.A. Brochero Cifuentes, I.J. Cabrillo, A. Calderon, M. Chamizo Llatas, S.H. Chuang, J. Duarte Campderros, M. Felcini[20], M. Fernandez, G. Gomez, J. Gonzalez Sanchez, C. Jorda, P. Lobelle Pardo, A. Lopez Virto, J. Marco, R. Marco, C. Martinez Rivero, F. Matorras, F.J. Munoz Sanchez, J. Piedra Gomez[21], T. Rodrigo, A. Ruiz Jimeno, L. Scodellaro, M. Sobron Sanudo, I. Vila, R. Vilar Cortabitarte

CERN, European Organization for Nuclear Research, Geneva, Switzerland
D. Abbaneo, E. Auffray, G. Auzinger, P. Baillon, A.H. Ball, D. Barney, A.J. Bell[22], D. Benedetti, C. Bernet[3], W. Bialas, P. Bloch, A. Bocci, S. Bolognesi, H. Breuker, G. Brona, K. Bunkowski, T. Camporesi, E. Cano, G. Cerminara, T. Christiansen, J.A. Coarasa Perez, B. Curé, D. D'Enterria, A. De Roeck, F. Duarte Ramos, A. Elliott-Peisert, B. Frisch, W. Funk, A. Gaddi, S. Gennai, G. Georgiou, H. Gerwig, D. Gigi, K. Gill, D. Giordano, F. Glege, R. Gomez-Reino Garrido, M. Gouzevitch, P. Govoni, S. Gowdy, L. Guiducci, M. Hansen, J. Harvey, J. Hegeman, B. Hegner, C. Henderson, G. Hesketh, H.F. Hoffmann, A. Honma, V. Innocente, P. Janot, E. Karavakis, P. Lecoq, C. Leonidopoulos, C. Lourenço, A. Macpherson, T. Mäki, L. Malgeri, M. Mannelli, L. Masetti, F. Meijers, S. Mersi, E. Meschi, R. Moser, M.U. Mozer, M. Mulders, E. Nesvold[1], M. Nguyen, T. Orimoto, L. Orsini, E. Perez, A. Petrilli, A. Pfeiffer, M. Pierini, M. Pimiä, G. Polese, A. Racz, G. Rolandi[23], T. Rommerskirchen, C. Rovelli[24], M. Rovere, H. Sakulin, C. Schäfer, C. Schwick, I. Segoni, A. Sharma, P. Siegrist, M. Simon, P. Sphicas[25], D. Spiga, M. Spiropulu[18], F. Stöckli, M. Stoye, P. Tropea, A. Tsirou, A. Tsyganov, G.I. Veres[12], P. Vichoudis, M. Voutilainen, W.D. Zeuner

Paul Scherrer Institut, Villigen, Switzerland
W. Bertl, K. Deiters, W. Erdmann, K. Gabathuler, R. Horisberger, Q. Ingram, H.C. Kaestli, S. König, D. Kotlinski, U. Langenegger, F. Meier, D. Renker, T. Rohe, J. Sibille[26], A. Starodumov[27]

Institute for Particle Physics, ETH Zurich, Zurich, Switzerland
P. Bortignon, L. Caminada[28], Z. Chen, S. Cittolin, G. Dissertori, M. Dittmar, J. Eugster, K. Freudenreich, C. Grab, A. Hervé, W. Hintz, P. Lecomte, W. Lustermann, C. Marchica[28], P. Martinez Ruiz del Arbol, P. Meridiani, P. Milenovic[29], F. Moortgat, P. Nef, F. Nessi-Tedaldi, L. Pape, F. Pauss, T. Punz, A. Rizzi, F.J. Ronga, M. Rossini, L. Sala, A.K. Sanchez, M.-C. Sawley, B. Stieger, L. Tauscher†, A. Thea, K. Theofilatos, D. Treille, C. Urscheler, R. Wallny[20], M. Weber, L. Wehrli, J. Weng

Universität Zürich, Zurich, Switzerland
E. Aguiló, C. Amsler, V. Chiochia, S. De Visscher, C. Favaro, M. Ivova Rikova, B. Millan Mejias, C. Regenfus, P. Robmann, A. Schmidt, H. Snoek, L. Wilke

National Central University, Chung-Li, Taiwan
Y.H. Chang, K.H. Chen, W.T. Chen, S. Dutta, A. Go, C.M. Kuo, S.W. Li, W. Lin, M.H. Liu, Z.K. Liu, Y.J. Lu, J.H. Wu, S.S. Yu

National Taiwan University (NTU), Taipei, Taiwan
P. Bartalini, P. Chang, Y.H. Chang, Y.W. Chang, Y. Chao, K.F. Chen, W.-S. Hou, Y. Hsiung, K.Y. Kao, Y.J. Lei, R.-S. Lu, J.G. Shiu, Y.M. Tzeng, M. Wang

Cukurova University, Adana, Turkey
A. Adiguzel, M.N. Bakirci[30], S. Cerci[31], C. Dozen, I. Dumanoglu, E. Eskut, S. Girgis, G. Gokbulut, Y. Guler, E. Gurpinar, I. Hos, E.E. Kangal, T. Karaman, A. Kayis Topaksu, A. Nart, G. Onengut, K. Ozdemir, S. Ozturk, A. Polatoz, K. Sogut[32], B. Tali, H. Topakli[30], D. Uzun, L.N. Vergili, M. Vergili, C. Zorbilmez

Middle East Technical University, Physics Department, Ankara, Turkey
I.V. Akin, T. Aliev, S. Bilmis, M. Deniz, H. Gamsizkan, A.M. Guler, K. Ocalan, A. Ozpineci, M. Serin, R. Sever, U.E. Surat, E. Yildirim, M. Zeyrek

Bogazici University, Istanbul, Turkey
M. Deliomeroglu, D. Demir[33], E. Gülmez, A. Halu, B. Isildak, M. Kaya[34], O. Kaya[34], S. Ozkorucuklu[35], N. Sonmez[36]

National Scientific Center, Kharkov Institute of Physics and Technology, Kharkov, Ukraine
L. Levchuk

University of Bristol, Bristol, United Kingdom
P. Bell, F. Bostock, J.J. Brooke, T.L. Cheng, E. Clement, D. Cussans, R. Frazier, J. Goldstein, M. Grimes, M. Hansen, D. Hartley, G.P. Heath, H.F. Heath, B. Huckvale, J. Jackson, L. Kreczko, S. Metson, D.M. Newbold[37], K. Nirunpong, A. Poll, S. Senkin, V.J. Smith, S. Ward

Rutherford Appleton Laboratory, Didcot, United Kingdom
L. Basso, K.W. Bell, A. Belyaev, C. Brew, R.M. Brown, B. Camanzi, D.J.A. Cockerill, J.A. Coughlan, K. Harder, S. Harper, B.W. Kennedy, E. Olaiya, D. Petyt, B.C. Radburn-Smith, C.H. Shepherd-Themistocleous, I.R. Tomalin, W.J. Womersley, S.D. Worm

Imperial College, London, United Kingdom
R. Bainbridge, G. Ball, J. Ballin, R. Beuselinck, O. Buchmuller, D. Colling, N. Cripps, M. Cutajar, G. Davies, M. Della Negra, J. Fulcher, D. Futyan, A. Guneratne Bryer, G. Hall, Z. Hatherell, J. Hays, G. Iles, G. Karapostoli, L. Lyons, A.-M. Magnan, J. Marrouche, R. Nandi, J. Nash, A. Nikitenko[27], A. Papageorgiou, M. Pesaresi, K. Petridis, M. Pioppi[38], D.M. Raymond, N. Rompotis, A. Rose, M.J. Ryan, C. Seez, P. Sharp, A. Sparrow, A. Tapper, S. Tourneur, M. Vazquez Acosta, T. Virdee, S. Wakefield, D. Wardrope, T. Whyntie

Brunel University, Uxbridge, United Kingdom
M. Barrett, M. Chadwick, J.E. Cole, P.R. Hobson, A. Khan, P. Kyberd, D. Leslie, W. Martin, I.D. Reid, L. Teodorescu

Baylor University, Waco, USA
K. Hatakeyama

Boston University, Boston, USA
T. Bose, E. Carrera Jarrin, A. Clough, C. Fantasia, A. Heister, J. St. John, P. Lawson, D. Lazic, J. Rohlf, D. Sperka, L. Sulak

Brown University, Providence, USA
A. Avetisyan, S. Bhattacharya, J.P. Chou, D. Cutts, A. Ferapontov, U. Heintz, S. Jabeen, G. Kukartsev, G. Landsberg, M. Narain, D. Nguyen, M. Segala, T. Speer, K.V. Tsang

University of California, Davis, Davis, USA
M.A. Borgia, R. Breedon, M. Calderon De La Barca Sanchez, D. Cebra, S. Chauhan, M. Chertok, J. Conway, P.T. Cox, J. Dolen, R. Erbacher, E. Friis, W. Ko, A. Kopecky, R. Lander, H. Liu, S. Maruyama, T. Miceli, M. Nikolic, D. Pellett, J. Robles, S. Salur, T. Schwarz, M. Searle, J. Smith, M. Squires, M. Tripathi, R. Vasquez Sierra, C. Veelken

University of California, Los Angeles, Los Angeles, USA
V. Andreev, K. Arisaka, D. Cline, R. Cousins, A. Deisher, J. Duris, S. Erhan, C. Farrell, J. Hauser, M. Ignatenko, C. Jarvis, C. Plager, G. Rakness, P. Schlein†, J. Tucker, V. Valuev

University of California, Riverside, Riverside, USA
J. Babb, R. Clare, J. Ellison, J.W. Gary, F. Giordano, G. Hanson, G.Y. Jeng, S.C. Kao, F. Liu, H. Liu, A. Luthra, H. Nguyen, G. Pasztor[39], A. Satpathy, B.C. Shen†, R. Stringer, J. Sturdy, S. Sumowidagdo, R. Wilken, S. Wimpenny

University of California, San Diego, La Jolla, USA
W. Andrews, J.G. Branson, G.B. Cerati, E. Dusinberre, D. Evans, F. Golf, A. Holzner, R. Kelley, M. Lebourgeois, J. Letts, B. Mangano, J. Muelmenstaedt, S. Padhi, C. Palmer, G. Petrucciani, H. Pi, M. Pieri, R. Ranieri, M. Sani, V. Sharma[1], S. Simon, Y. Tu, A. Vartak, F. Würthwein, A. Yagil

University of California, Santa Barbara, Santa Barbara, USA
D. Barge, R. Bellan, C. Campagnari, M. D'Alfonso, T. Danielson, K. Flowers, P. Geffert, J. Incandela, C. Justus, P. Kalavase, S.A. Koay, D. Kovalskyi, V. Krutelyov, S. Lowette, N. Mccoll, V. Pavlunin, F. Rebassoo, J. Ribnik, J. Richman, R. Rossin, D. Stuart, W. To, J.R. Vlimant

California Institute of Technology, Pasadena, USA
A. Bornheim, J. Bunn, Y. Chen, M. Gataullin, D. Kcira, V. Litvine, Y. Ma, A. Mott, H.B. Newman, C. Rogan, V. Timciuc, P. Traczyk, J. Veverka, R. Wilkinson, Y. Yang, R.Y. Zhu

Carnegie Mellon University, Pittsburgh, USA
B. Akgun, R. Carroll, T. Ferguson, Y. Iiyama, D.W. Jang, S.Y. Jun, Y.F. Liu, M. Paulini, J. Russ, N. Terentyev, H. Vogel, I. Vorobiev

University of Colorado at Boulder, Boulder, USA
J.P. Cumalat, M.E. Dinardo, B.R. Drell, C.J. Edelmaier, W.T. Ford, B. Heyburn, E. Luiggi Lopez, U. Nauenberg, J.G. Smith, K. Stenson, K.A. Ulmer, S.R. Wagner, S.L. Zang

Cornell University, Ithaca, USA
L. Agostino, J. Alexander, A. Chatterjee, S. Das, N. Eggert, L.J. Fields, L.K. Gibbons, B. Heltsley, W. Hopkins, A. Khukhunaishvili, B. Kreis, V. Kuznetsov, G. Nicolas Kaufman, J.R. Patterson, D. Puigh, D. Riley, A. Ryd, X. Shi, W. Sun, W.D. Teo, J. Thom, J. Thompson, J. Vaughan, Y. Weng, L. Winstrom, P. Wittich

Fairfield University, Fairfield, USA
A. Biselli, G. Cirino, D. Winn

Fermi National Accelerator Laboratory, Batavia, USA
S. Abdullin, M. Albrow, J. Anderson, G. Apollinari, M. Atac, J.A. Bakken, S. Banerjee, L.A.T. Bauerdick, A. Beretvas, J. Berryhill, P.C. Bhat, I. Bloch, F. Borcherding, K. Burkett, J.N. Butler, V. Chetluru, H.W.K. Cheung, F. Chlebana, S. Cihangir, M. Demarteau, D.P. Eartly, V.D. Elvira, S. Esen, I. Fisk, J. Freeman, Y. Gao, E. Gottschalk, D. Green, K. Gunthoti, O. Gutsche, A. Hahn, J. Hanlon, R.M. Harris, J. Hirschauer, B. Hooberman, E. James, H. Jensen, M. Johnson, U. Joshi, R. Khatiwada, B. Kilminster, B. Klima, K. Kousouris, S. Kunori, S. Kwan, P. Limon, R. Lipton, J. Lykken, K. Maeshima, J.M. Marraffino, D. Mason, P. McBride, T. McCauley, T. Miao, K. Mishra, S. Mrenna, Y. Musienko[40], C. Newman-Holmes, V. O'Dell, S. Popescu[41], R. Pordes, O. Prokofyev, N. Saoulidou, E. Sexton-Kennedy, S. Sharma, A. Soha, W.J. Spalding, L. Spiegel, P. Tan, L. Taylor, S. Tkaczyk, L. Uplegger, E.W. Vaandering, R. Vidal, J. Whitmore, W. Wu, F. Yang, F. Yumiceva, J.C. Yun

University of Florida, Gainesville, USA
D. Acosta, P. Avery, D. Bourilkov, M. Chen, G.P. Di Giovanni, D. Dobur, A. Drozdetskiy, R.D. Field, M. Fisher, Y. Fu, I.K. Furic, J. Gartner, S. Goldberg, B. Kim, S. Klimenko, J. Konigsberg, A. Korytov, A. Kropivnitskaya, T. Kypreos, K. Matchev, G. Mitselmakher, L. Muniz, Y. Pakhotin, C. Prescott, R. Remington, M. Schmitt, B. Scurlock, P. Sellers, N. Skhirtladze, D. Wang, J. Yelton, M. Zakaria

Florida International University, Miami, USA
C. Ceron, V. Gaultney, L. Kramer, L.M. Lebolo, S. Linn, P. Markowitz, G. Martinez, J.L. Rodriguez

Florida State University, Tallahassee, USA
T. Adams, A. Askew, D. Bandurin, J. Bochenek, J. Chen, B. Diamond, S.V. Gleyzer, J. Haas, S. Hagopian, V. Hagopian, M. Jenkins, K.F. Johnson, H. Prosper, S. Sekmen, V. Veeraraghavan

Florida Institute of Technology, Melbourne, USA
M.M. Baarmand, B. Dorney, S. Guragain, M. Hohlmann, H. Kalakhety, R. Ralich, I. Vodopiyanov

University of Illinois at Chicago (UIC), Chicago, USA
M.R. Adams, I.M. Anghel, L. Apanasevich, Y. Bai, V.E. Bazterra, R.R. Betts, J. Callner, R. Cavanaugh, C. Dragoiu, E.J. Garcia-Solis, C.E. Gerber, D.J. Hofman, S. Khalatyan, F. Lacroix, C. O'Brien, C. Silvestre, A. Smoron, D. Strom, N. Varelas

The University of Iowa, Iowa City, USA
U. Akgun, E.A. Albayrak, B. Bilki, K. Cankocak[42], W. Clarida, F. Duru, C.K. Lae, E. McCliment, J.-P. Merlo, H. Mermerkaya, A. Mestvirishvili, A. Moeller, J. Nachtman, C.R. Newsom, E. Norbeck, J. Olson, Y. Onel, F. Ozok, S. Sen, J. Wetzel, T. Yetkin, K. Yi

Johns Hopkins University, Baltimore, USA
B.A. Barnett, B. Blumenfeld, A. Bonato, C. Eskew, D. Fehling, G. Giurgiu, A.V. Gritsan, Z.J. Guo, G. Hu, P. Maksimovic, S. Rappoccio, M. Swartz, N.V. Tran, A. Whitbeck

The University of Kansas, Lawrence, USA
P. Baringer, A. Bean, G. Benelli, O. Grachov, M. Murray, D. Noonan, V. Radicci, S. Sanders, J.S. Wood, V. Zhukova

Kansas State University, Manhattan, USA
T. Bolton, I. Chakaberia, A. Ivanov, M. Makouski, Y. Maravin, S. Shrestha, I. Svintradze, Z. Wan

Lawrence Livermore National Laboratory, Livermore, USA
J. Gronberg, D. Lange, D. Wright

University of Maryland, College Park, USA
A. Baden, M. Boutemeur, S.C. Eno, D. Ferencek, J.A. Gomez, N.J. Hadley, R.G. Kellogg, M. Kirn, Y. Lu, A.C. Mignerey, K. Rossato, P. Rumerio, F. Santanastasio, A. Skuja, J. Temple, M.B. Tonjes, S.C. Tonwar, E. Twedt

Massachusetts Institute of Technology, Cambridge, USA
B. Alver, G. Bauer, J. Bendavid, W. Busza, E. Butz, I.A. Cali, M. Chan, V. Dutta, P. Everaerts, G. Gomez Ceballos, M. Goncharov, K.A. Hahn, P. Harris, Y. Kim, M. Klute, Y.-J. Lee, W. Li, C. Loizides, P.D. Luckey, T. Ma, S. Nahn, C. Paus, D. Ralph, C. Roland, G. Roland, M. Rudolph, G.S.F. Stephans, K. Sumorok, K. Sung, E.A. Wenger, S. Xie, M. Yang, Y. Yilmaz, A.S. Yoon, M. Zanetti

University of Minnesota, Minneapolis, USA
P. Cole, S.I. Cooper, P. Cushman, B. Dahmes, A. De Benedetti, P.R. Dudero, G. Franzoni, J. Haupt, K. Klapoetke, Y. Kubota, J. Mans, V. Rekovic, R. Rusack, M. Sasseville, A. Singovsky

University of Mississippi, University, USA
L.M. Cremaldi, R. Godang, R. Kroeger, L. Perera, R. Rahmat, D.A. Sanders, D. Summers

University of Nebraska-Lincoln, Lincoln, USA
K. Bloom, S. Bose, J. Butt, D.R. Claes, A. Dominguez, M. Eads, J. Keller, T. Kelly, I. Kravchenko, J. Lazo-Flores, C. Lundstedt, H. Malbouisson, S. Malik, G.R. Snow

State University of New York at Buffalo, Buffalo, USA
U. Baur, A. Godshalk, I. Iashvili, A. Kharchilava, A. Kumar, S.P. Shipkowski, K. Smith

Northeastern University, Boston, USA
G. Alverson, E. Barberis, D. Baumgartel, O. Boeriu, M. Chasco, K. Kaadze, S. Reucroft, J. Swain, D. Wood, J. Zhang

Northwestern University, Evanston, USA
A. Anastassov, A. Kubik, N. Odell, R.A. Ofierzynski, B. Pollack, A. Pozdnyakov, M. Schmitt, S. Stoynev, M. Velasco, S. Won

University of Notre Dame, Notre Dame, USA
L. Antonelli, D. Berry, M. Hildreth, C. Jessop, D.J. Karmgard, J. Kolb, T. Kolberg, K. Lannon, W. Luo, S. Lynch, N. Marinelli, D.M. Morse, T. Pearson, R. Ruchti, J. Slaunwhite, N. Valls, J. Warchol, M. Wayne, J. Ziegler

The Ohio State University, Columbus, USA
B. Bylsma, L.S. Durkin, J. Gu, C. Hill, P. Killewald, K. Kotov, T.Y. Ling, M. Rodenburg, G. Williams

Princeton University, Princeton, USA
N. Adam, E. Berry, P. Elmer, D. Gerbaudo, V. Halyo, P. Hebda, A. Hunt, J. Jones, E. Laird, D. Lopes Pegna, D. Marlow, T. Medvedeva, M. Mooney, J. Olsen, P. Piroué, X. Quan, H. Saka, D. Stickland, C. Tully, J.S. Werner, A. Zuranski

University of Puerto Rico, Mayaguez, USA
J.G. Acosta, X.T. Huang, A. Lopez, H. Mendez, S. Oliveros, J.E. Ramirez Vargas, A. Zatserklyaniy

Purdue University, West Lafayette, USA
E. Alagoz, V.E. Barnes, G. Bolla, L. Borrello, D. Bortoletto, A. Everett, A.F. Garfinkel, Z. Gecse, L. Gutay, Z. Hu, M. Jones, O. Koybasi, A.T. Laasanen, N. Leonardo, C. Liu, V. Maroussov, P. Merkel, D.H. Miller, N. Neumeister, K. Potamianos, I. Shipsey, D. Silvers, A. Svyatkovskiy, H.D. Yoo, J. Zablocki, Y. Zheng

Purdue University Calumet, Hammond, USA
P. Jindal, N. Parashar

Rice University, Houston, USA
C. Boulahouache, V. Cuplov, K.M. Ecklund, F.J.M. Geurts, J.H. Liu, J. Morales, B.P. Padley, R. Redjimi, J. Roberts, J. Zabel

University of Rochester, Rochester, USA
B. Betchart, A. Bodek, Y.S. Chung, R. Covarelli, P. de Barbaro, R. Demina, Y. Eshaq, H. Flacher,

A. Garcia-Bellido, P. Goldenzweig, Y. Gotra, J. Han, A. Harel, D.C. Miner, D. Orbaker, G. Petrillo, D. Vishnevskiy, M. Zielinski

The Rockefeller University, New York, USA
A. Bhatti, L. Demortier, K. Goulianos, G. Lungu, C. Mesropian, M. Yan

Rutgers, the State University of New Jersey, Piscataway, USA
O. Atramentov, A. Barker, D. Duggan, Y. Gershtein, R. Gray, E. Halkiadakis, D. Hidas, D. Hits, A. Lath, S. Panwalkar, R. Patel, A. Richards, K. Rose, S. Schnetzer, S. Somalwar, R. Stone, S. Thomas

University of Tennessee, Knoxville, USA
G. Cerizza, M. Hollingsworth, S. Spanier, Z.C. Yang, A. York

Texas A&M University, College Station, USA
J. Asaadi, R. Eusebi, J. Gilmore, A. Gurrola, T. Kamon, V. Khotilovich, R. Montalvo, C.N. Nguyen, I. Osipenkov, J. Pivarski, A. Safonov, S. Sengupta, A. Tatarinov, D. Toback, M. Weinberger

Texas Tech University, Lubbock, USA
N. Akchurin, C. Bardak, J. Damgov, C. Jeong, K. Kovitanggoon, S.W. Lee, P. Mane, Y. Roh, A. Sill, I. Volobouev, R. Wigmans, E. Yazgan

Vanderbilt University, Nashville, USA
E. Appelt, E. Brownson, D. Engh, C. Florez, W. Gabella, W. Johns, P. Kurt, C. Maguire, A. Melo, P. Sheldon, J. Velkovska

University of Virginia, Charlottesville, USA
M.W. Arenton, M. Balazs, S. Boutle, M. Buehler, S. Conetti, B. Cox, B. Francis, R. Hirosky, A. Ledovskoy, C. Lin, C. Neu, R. Yohay

Wayne State University, Detroit, USA
S. Gollapinni, R. Harr, P.E. Karchin, P. Lamichhane, M. Mattson, C. Milstène, A. Sakharov

University of Wisconsin, Madison, USA
M. Anderson, M. Bachtis, J.N. Bellinger, D. Carlsmith, S. Dasu, J. Efron, L. Gray, K.S. Grogg, M. Grothe, R. Hall-Wilton[1], M. Herndon, P. Klabbers, J. Klukas, A. Lanaro, C. Lazaridis, J. Leonard, D. Lomidze, R. Loveless, A. Mohapatra, D. Reeder, I. Ross, A. Savin, W.H. Smith, J. Swanson, M. Weinberg

†: Deceased
1: Also at CERN, European Organization for Nuclear Research, Geneva, Switzerland
2: Also at Universidade Federal do ABC, Santo Andre, Brazil
3: Also at Laboratoire Leprince-Ringuet, Ecole Polytechnique, IN2P3-CNRS, Palaiseau, France
4: Also at Suez Canal University, Suez, Egypt
5: Also at Fayoum University, El-Fayoum, Egypt
6: Also at Soltan Institute for Nuclear Studies, Warsaw, Poland
7: Also at Massachusetts Institute of Technology, Cambridge, USA
8: Also at Université de Haute-Alsace, Mulhouse, France
9: Also at Brandenburg University of Technology, Cottbus, Germany
10: Also at Moscow State University, Moscow, Russia
11: Also at Institute of Nuclear Research ATOMKI, Debrecen, Hungary
12: Also at Eötvös Loránd University, Budapest, Hungary
13: Also at Tata Institute of Fundamental Research - HECR, Mumbai, India

14: Also at University of Visva-Bharati, Santiniketan, India
15: Also at Facoltà Ingegneria Università di Roma "La Sapienza", Roma, Italy
16: Also at Università della Basilicata, Potenza, Italy
17: Also at Laboratori Nazionali di Legnaro dell' INFN, Legnaro, Italy
18: Also at California Institute of Technology, Pasadena, USA
19: Also at Faculty of Physics of University of Belgrade, Belgrade, Serbia
20: Also at University of California, Los Angeles, Los Angeles, USA
21: Also at University of Florida, Gainesville, USA
22: Also at Université de Genève, Geneva, Switzerland
23: Also at Scuola Normale e Sezione dell' INFN, Pisa, Italy
24: Also at INFN Sezione di Roma; Università di Roma "La Sapienza", Roma, Italy
25: Also at University of Athens, Athens, Greece
26: Also at The University of Kansas, Lawrence, USA
27: Also at Institute for Theoretical and Experimental Physics, Moscow, Russia
28: Also at Paul Scherrer Institut, Villigen, Switzerland
29: Also at University of Belgrade, Faculty of Physics and Vinca Institute of Nuclear Sciences, Belgrade, Serbia
30: Also at Gaziosmanpasa University, Tokat, Turkey
31: Also at Adiyaman University, Adiyaman, Turkey
32: Also at Mersin University, Mersin, Turkey
33: Also at Izmir Institute of Technology, Izmir, Turkey
34: Also at Kafkas University, Kars, Turkey
35: Also at Suleyman Demirel University, Isparta, Turkey
36: Also at Ege University, Izmir, Turkey
37: Also at Rutherford Appleton Laboratory, Didcot, United Kingdom
38: Also at INFN Sezione di Perugia; Università di Perugia, Perugia, Italy
39: Also at KFKI Research Institute for Particle and Nuclear Physics, Budapest, Hungary
40: Also at Institute for Nuclear Research, Moscow, Russia
41: Also at Horia Hulubei National Institute of Physics and Nuclear Engineering (IFIN-HH), Bucharest, Romania
42: Also at Istanbul Technical University, Istanbul, Turkey